Agricultural and Forest Meteorology 171–172 (2013) 31–45

Contents lists available at SciVerse ScienceDirect

Agricultural and Forest Meteorology

journal homepage: www.elsevier.com/locate/agrformet

Use of change-point detection for friction–velocity threshold evaluation in eddy-covariance studies

A.G. Barr[a,*], A.D. Richardson[b], D.Y. Hollinger[c], D. Papale[d], M.A. Arain[e], T.A. Black[f], G. Bohrer[g], D. Dragoni[h], M.L. Fischer[i], L. Gu[j], B.E. Law[k], H.A. Margolis[l], J.H. McCaughey[m], J.W. Munger[n], W. Oechel[o], K. Schaeffer[p]

[a] Climate Research Division, Environment Canada, 11 Innovation Blvd., Saskatoon, SK, Canada S7N 3H5
[b] Harvard University, Department of Organismic and Evolutionary Biology, Harvard University Herbaria, 22 Divinity Avenue, Cambridge, MA 02138, USA
[c] USDA Forest Service, Northern Research Station, 271 Mast Road, Durham, NH 03824, USA
[d] Department for Innovation in Biological, Agro-food and Forest Systems (DIBAF), University of Tuscia, Viea San Camillo Ed Lellis, Viterbo 01100, Italy
[e] School of Geography and Earth Sciences, McMaster University, Hamilton, ON, Canada L8S 4K1
[f] Faculty of Land and Food Systems, University of British Columbia, Vancouver, BC, Canada V6T 1Z4
[g] Department of Civil, Environmental and Geodetic Engineering, The Ohio State University, 2070 Neil Ave., Columbus, OH 43210, USA
[h] Department of Geography, Indiana University, Bloomington, IN 47405, USA
[i] Environmental Energy Technologies Division, Lawrence Berkeley National Laboratory, Berkeley, CA 94720, USA
[j] Environmental Sciences Division, Oak Ridge National Laboratory, Oak Ridge, TN 37831-6335, USA
[k] Oregon State University, 328 Richardson Hall, Corvallis, OR 97331, USA
[l] Centre d'Étude de la Forêt, Laval University, Quebec City, QC, Canada G1V 0A6
[m] Department of Geography, Queen's University, Kingston, ON, Canada K7L 3N6
[n] School of Engineering and Applied Sciences and Department of Earth and Planetary Sciences, Harvard University, Cambridge, MA 02138, USA
[o] Department of Biology and the Global Change Research Group, San Diego State University, San Diego, CA 92182, USA
[p] National Snow and Ice Data Center, Cooperative Institute for Research in Environmental Sciences, University of Colorado at Boulder, Boulder, CO 80309, USA

ARTICLE INFO

Article history:
Received 26 May 2012
Received in revised form 10 October 2012
Accepted 30 November 2012

Keywords:
Eddy-covariance
Friction–velocity filters
Uncertainty
Change-point detection

ABSTRACT

The eddy-covariance method often underestimates fluxes under stable, low-wind conditions at night when turbulence is not well developed. The most common approach to resolve the problem of nighttime flux underestimation is to identify and remove the deficit periods using friction–velocity (u_*) threshold filters (u_*^{Th}). This study modifies an accepted method for u_*^{Th} evaluation by incorporating change-point-detection techniques. The original and modified methods are evaluated at 38 sites as part of the North American Carbon Program (NACP) site-level synthesis. At most sites, the modified method produced u_*^{Th} estimates that were higher and less variable than the original method. It also provided an objective method to identify sites that lacked a u_*^{Th} response. The modified u_*^{Th} estimates were robust and comparable among years. Inter-annual u_*^{Th} differences were small, so that a single u_*^{Th} value was warranted at most sites. No variation in the u_*^{Th} was observed by time of day (dusk versus mid or late night), however, a few sites showed significant u_*^{Th} variation with time of year. Among-site variation in the u_*^{Th} was strongly related to canopy height and the mean annual nighttime u_*. The modified u_*^{Th} estimates excluded a high fraction of nighttime data – 61% on average. However, the negative impact of the high exclusion rate on annual net ecosystem production (NEP) was small compared to the larger impact of underestimating the u_*^{Th}. Compared to the original method, the higher u_*^{Th} estimates from the modified method caused a mean 8% reduction in annual NEP across all site-years, and a mean 7% increase in total ecosystem respiration (R_e). The modified method also reduced the u_*^{Th}-related uncertainties in annual NEP and R_e by more than 50%. These results support the use of u_*^{Th} filters as a pragmatic solution to a complex problem.

* Corresponding author. Fax: +1 306 975 6516.
E-mail addresses: alan.barr@ec.gc.ca (A.G. Barr), arichardson@oeb.harvard.edu (A.D. Richardson), dhollinger@fs.fed.us (D.Y. Hollinger), darpap@unitus.it (D. Papale), arainm@mcmaster.ca (M.A. Arain), andrew.black@ubc.ca (T.A. Black), bohrer.17@osu.edu (G. Bohrer), ddragoni@indiana.edu (D. Dragoni), mlfischer@lbl.gov (M.L. Fischer), lianhong-gu@ornl.gov (L. Gu), bev.law@oregonstate.edu (B.E. Law), hank.margolis@sbf.ulaval.ca (H.A. Margolis), mccaughe@queensu.ca (J.H. McCaughey), jwmunger@seas.harvard.edu (J.W. Munger), oechel@sunstroke.sdsu.edu (W. Oechel), kevin.schaefer@nsidc.org (K. Schaeffer).

0168-1923/$ – see front matter © 2012 A.G. Barr. Published by Elsevier B.V. All rights reserved.
http://dx.doi.org/10.1016/j.agrformet.2012.11.023

1. Introduction

The eddy-covariance (EC) method has gained worldwide acceptance as a basic tool in the study of the terrestrial carbon cycle (Baldocchi et al., 2001). At present flux tower networks are operational on seven continents and in all major ecozones (Baldocchi, 2008). EC flux data sets from diverse ecosystems are producing new insights into the spatial distribution of terrestrial carbon sources and sinks (Valentini et al., 2000; Janssens et al., 2001; Beer et al., 2010), the response of the carbon cycle to climate variability and change (Reichstein et al., 2007a,b; Piao et al., 2008; Richardson et al., 2010), ecophysiological processes and their climatic controls (Irvine et al., 2005; Mahecha et al., 2010), and the role of disturbance and land-use change (Law, 2006; Davis, 2008; Amiro et al., 2010). From their inception, flux-tower networks have played a foundational role in the development of global carbon cycle models (Sellers et al., 1997; Running et al., 1999; Schwalm et al., 2010).

However, the EC method is not without problems. It is based on turbulent transport across the plane of flux measurement and storage changes below the measurement plane. At night, EC systems located above terrestrial ecosystems may report little or no carbon dioxide exchange even when such exchanges are known to be occurring. These flux deficits occur under stable, low-wind conditions when turbulence is not well developed (Hollinger et al., 1994; Goulden et al., 1996; Aubinet et al., 2000; Massman and Lee, 2002; Gu et al., 2005; Barr et al., 2006). The "nighttime problem" has long been recognized (Anderson et al., 1984; Ohtaki, 1984) but its cause and resolution remain an active area of research (Staebler and Fitzjarrald, 2004; van Gorsel et al., 2007; Yi et al., 2008; Aubinet et al., 2010; Gu et al., 2012). Aubinet (2008) identified two primary causes of nighttime EC flux deficits: intermittent turbulence and advective transport. The former should be fully resolvable through data quality screening, using e.g. stationarity (Mahrt, 1998) and integral turbulence tests (Foken and Wichura, 1996). The latter is more difficult to resolve. Although most implementations of the EC method assume that scalar transport by horizontal and vertical advection is negligible, this assumption is often violated, particularly at night when calm winds and stable stratification promote stationary two- and three-dimensional flow regimes (Aubinet, 2008). Examples include drainage flows (Aubinet et al., 2003; Staebler and Fitzjarrald, 2005; Belcher et al., 2008; Feigenwinter et al., 2008), venting over boreal lakes (Sun et al., 1998), and land and sea breezes (Sun et al., 2006). The result is that the EC turbulent flux plus storage change below the EC sensors under-measures the total exchange.

Another plausible explanation of flux under-measurement by EC was recently proposed by Gu et al. (2012) who revisited the storage-change term in the WPL analysis (Webb et al., 1980). They identified a shortcoming in the storage-change calculation during non-steady-state conditions, such as often occur during calm nights. Their "effective change in storage" term corrects for the shortcoming. A multi-site analysis is needed to evaluate the degree to which this correction reduces the problems of flux under-measurement during calm nights.

Nighttime flux deficits are a major source of uncertainty and potential bias in EC measurements of net ecosystem exchange (NEE). Because they affect the magnitude of the day – night difference, they in turn affect the size of the daily and annual NEE integrals (Goulden et al., 1996; Barford et al., 2001) and the partitioning of NEE into ecosystem respiration (R_e) and gross primary production (P) (Falge et al., 2001; Barr et al., 2006; Papale et al., 2006). The uncertainties associated with nighttime deficits typically overwhelm other methodological sources of uncertainty such as coordinate rotation, instrument noise, or calibration errors (Morgenstern et al., 2004; Loescher et al., 2006).

Solutions to the nighttime problem fall into two categories: advection estimation; and data filtering and gap filling. The most fundamental solution is to include horizontal and vertical advection in the flux calculations, either through direct measurement (e.g., Feigenwinter et al., 2004; Staebler and Fitzjarrald, 2004; Marcolla et al., 2005; Aubinet et al., 2005, 2010; Heinesch et al., 2008; Leuning et al., 2008; Montagnani et al., 2009), measurement supplemented by modeling (Canepa et al., 2010), or parameterizing the advective fluxes based on measurements from focused field campaigns (Yi et al., 2008). However, the direct quantification of advective fluxes is so data intensive and the associated uncertainties are so large that it is not presently viable to include advection in routine EC implementations (Finnigan, 2008; Aubinet et al., 2010; Canepa et al., 2010).

In the absence of reliable advection measurements, several data filtering approaches have been developed to resolve the problem of nighttime flux under-estimation. The most common, originally proposed by Goulden et al. (1996), is the application of friction velocity (u_*) filters that reject nighttime NEE when u_* falls below a critical threshold (u_*^{Th}) (Aubinet et al., 2000; Barr et al., 2006). Conceptually, this method assumes that the effects of advection are negligible during periods with sufficient turbulent kinetic energy (above the u_*^{Th}). The data gaps created by u_*^{Th} filtering are filled using a variety of gap-filling methods (Moffat et al., 2007). The use of u_* filters has been widely criticized as a gross over-simplification (Acevedo et al., 2009; van Gorsel et al., 2009). Other screening alternatives include: σ_w filters, where σ_w is the standard deviation of the vertical velocity (Black et al., 1996; Acevedo et al., 2009); screening by the buoyancy forcing fraction or stability class (Staebler and Fitzjarrald, 2004; Hollinger et al., 2004; Barr et al., 2006); and limiting the acceptable nighttime data to the NEE maximum that occurs soon after sunset, when the advective fluxes are assumed to be negligible (van Gorsel et al., 2007, 2008).

When the u_*^{Th} approach is used, the u_*^{Th} filter must be evaluated on a site-by-site basis from the NEE versus u_* relationship. Algorithms for automated u_*^{Th} evaluation are needed in multi-site synthesis studies to minimize differences in the subjective selection of the threshold and often employ moving-point tests (MPT) (Saleska et al., 2003; Gu et al., 2005; Papale et al., 2006) whereby a horizontal asymptote in a $y = f(x)$ relationship is determined by comparing each y value with the mean of the y values at higher x. An attractive but previously untested alternative to MPT is change-point detection (CPD), a technique that is widely used to detect temporal discontinuities in climatic data (Solow, 1987; Lund and Reeves, 2002; Wang, 2003). CPD is well suited to u_*^{Th} evaluation; it provides an objective, robust procedure to determine if the relationship between u_* and NEE changes at some value of u_* (the change-point or u_*^{Th}) and includes a test of statistical significance.

This study compares the MPT implementation of Reichstein et al. (2005) modified by Papale et al. (2006) with the CPD methodology of Lund and Reeves (2002) and Wang (2003), modified for u_*^{Th} evaluation by adding continuity and slope constraints (Section 2) and implemented within the basic framework of Papale et al. (2006). The comparison is part of the North American Carbon Program (NACP) Site Synthesis and uses data from 38 North American flux-tower sites. The NACP Site Synthesis addresses the question: Are eddy-covariance measurements and carbon-cycle model estimates of carbon fluxes consistent with each other, given uncertainties in both data and models – and if not, why? Within that broad goal, the particular objectives of this study are: to assess the suitability of the u_*^{Th} approach across a wide variety of sites; to improve automated u_*^{Th} evaluation using CPD techniques; to examine temporal variation in the u_*^{Th}, diurnally, seasonally and among years; to relate the u_*^{Th} to site characteristics; and to characterize the uncertainty in annual CO_2 fluxes associated with uncertainty in the u_*^{Th}. The

study is part of a larger effort to characterize flux uncertainties at NACP sites.

2. Methods

2.1. Sites and data

The NACP sites used in this study span a broad range of plant functional types, including: mature forests (evergreen needleleaf, deciduous broadleaf, and mixedwood); juvenile forests; crop lands; grasslands; wetlands; savannah; and shrublands. Salient features, by site, are given in Table 1. The sites were selected based on biome reprentativeness, data completeness and data quality.

EC fluxes of NEE and u_* were retrieved from the Canadian Carbon Program's Data Information System for Canadian sites and the Ameriflux data base for USA sites. In addition to data quality screening by the site investigators, we applied some coarse outlier removal prior to the u_*^{Th} analysis, following Papale et al. (2006). NEE was calculated as the sum of the turbulent and storage fluxes, with the storage flux based on CO_2 profile measurements when available and on a single CO_2 measurement at the EC instrument level when CO_2 profile measurements were unavailable. In this paper, we will use the term net ecosystem exchange (NEE, $\mu mol\, m^{-2}\, s^{-1}$) to denote the measured 30- or 60-min fluxes following the meteorological convention of a positive sign for carbon release to the atmosphere, and the term net ecosystem production (NEP, $g\, C\, m^{-2}\, y^{-1}$) to denote integrated fluxes at the annual time scale using the ecological convention of a positive sign for carbon uptake by the ecosystem.

2.2. Original and modified u_*^{Th} methods

We used a modification of the Papale et al. MPT (2006) method to determine the u_*^{Th} and its uncertainty. The original MPT method (Papale et al., 2006) stratifies each site-year of data into four ($n_S = 4$) three-month long seasons (JFM, AMJ, JAS, and OND) and each season into a number of air temperature classes ($n_T = 7$). The u_*^{Th} is then evaluated independently for each of the $n_S * n_T$ strata. The purpose of stratification is to minimize the possibility that the NEE versus u_* relationship is confounded by seasonal and temperature dependencies. Within each strata, the u_*^{Th} is evaluated as follows. Binned means of nighttime NEE and u_* are computed for 20 equally-sized u_* classes (where n_B, the number of bins, was set to 20 for pragmatic reasons). The u_*^{Th} is then identified by MPT, comparing each binned NEE value with the mean of the binned NEE values at higher u_* (either from the next 10 u_* bins or from all higher u_* bins, whichever is less). The MPT algorithm assigns u_*^{Th} as the lowest u_* value with NEE that exceeds 99% of the mean NEE at higher u_*. The annual u_*^{Th} is estimated in two steps, first computing the median u_*^{Th} across the temperature strata within each season, then selecting the maximum of the four seasonal medians.

We modified the original Papale et al. (2006) procedure in three ways: replacing the MPT threshold-detection algorithm with a CPD technique (Section 2.3); modifying the stratification and binning procedures; and using a simple average to calculate the annual u_*^{Th} from the $n_S * n_T$ strata, rather than the maximum of the four seasonal medians. To improve the stability of the u_*^{Th} estimates, we modified the seasonal stratification using temporal moving windows (with $n_S = 7$–17 seasonal moving windows, depending on the number of data, and $n_T = 4$ temperature classes in each window), with 50% overlap between adjacent windows to increase the temporal resolution and sample size. We also increased the minimum number of data points within each of the $n_S * n_T$ strata to 50 bins of 5 points per bin for 30-min flux data and 50 bins of 3 points per bin for 60-min flux data, based on the results of algorithm testing with synthetic data (Sections 2.6 and 3.2). The CPD technique included objective criteria to detect cases that lacked a u_*^{Th} response (Sections 2.3 and 2.4). Uncertainty was estimated by bootstrapping, using the procedure outlined by Papale et al. (2006).

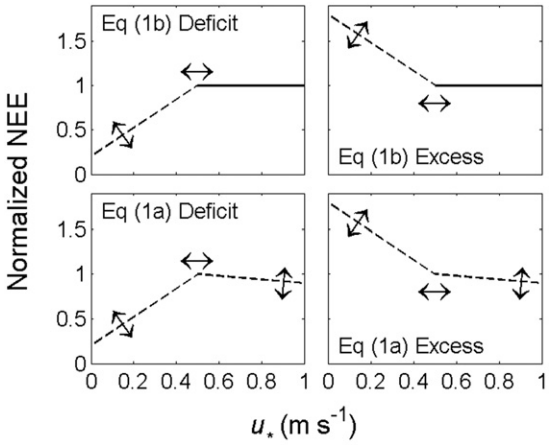

Fig. 1. Examples of the operational (Eq. (1b), upper panels) and diagnostic (Eq. (1a), lower panels) change-point models, in deficit mode (left panels) and excess mode (right panels). NEE has been normalized to one at the change point. The arrows indicate variation in model parameters.

2.3. Change-point detection

Solow (1987) introduced a method to identify an unknown change-point x_c in an (x, y) data series of n values using two-phase linear regression:

$$y_i = \begin{cases} a_0 + a_1 x_i + \varepsilon, & 1 \le i \le c \\ a_0 + a_1 x_c + a_2 (x_i - x_c) + \varepsilon, & c < i \le n \end{cases} \quad (1a)$$

where x_c denotes the change-point. Equation (1a) imposes a continuity constraint at the change-point; we modified Eq. (1a) for u_*^{Th} detection by adding a zero-slope constraint above x_c:

$$y_i = \begin{cases} b_0 + b_1 x_i + \varepsilon, & 1 \le i \le c \\ b_0 + b_1 x_c + \varepsilon, & c < i \le n \end{cases} \quad (1b)$$

which reduces the number of parameters from $n_a = 3$ to $n_b = 2$. In this study, Eq. (1b) is used to evaluate the u_*^{Th} whereas Eq. (1a) is used as a diagnostic tool to assess the suitability of a u_*^{Th} filter. The diagnostic Eq. (1a) and operational Eq. (1b) models are illustrated in Fig. 1, each in two possible modes: the more common NEE deficit mode (with NEE deficits at low u_*, i.e. $a_1 > a_2$ Eq. (1a) or $b_1 > 0$ Eq. (1b)) and the less common NEE excess mode (with NEE excesses at low u_*, i.e. $a_1 < a_2$ Eq. (1a) or $b_1 < 0$ Eq. (1b)).

The most probable value for x_c (Solow, 1987; Wang, 2003) is the one that maximizes F_c

$$F_{\max} = \max_{2 \le c \le (n-1)} (F_c)$$

where F_c is the F score calculated for each value of c from 2 to $n-1$. $F_{\max}$ compares the goodness of fit of the change-point model (Eqs. (1a) or (1b)) with a reduced null-hypothesis model that lacks a change-point. The null-hypothesis models are, for Eq. (1a):

$$y = \alpha_0 + \alpha_1 x + \varepsilon \quad (2a)$$

and for Eq. (1b):

$$y = \beta_0 + \varepsilon \quad (2b)$$

Table 1
Sites from the NACP site synthesis.

Site	Site code	Site letter	Years	Latitude (°N)	Longitude (°W)	IGBP Class[a]	Canopy height (m)	Reference
BC Campbell River Douglas-fir 1949	CACa1	c	1998–2006	49.867	125.334	ENF	32.5	Morgenstern et al. (2004)
BC Campbell River Douglas-fir Harvested 2000	CACa2	d	2001–2006	49.870	125.291	ENF	0.8	Humphreys et al. (2006)
BC Campbell River Douglas-fir Harvested 1988	CACa3	e	2002–2006	49.535	124.900	ENF	7.6	Humphreys et al. (2006)
ON Groundhog River Mixed Wood	CAGro	g	2004–2006	48.217	82.156	MF	14.4	McCaughey et al. (2006)
AB Lethbridge Grassland	CALet	l	1999–2007	49.43	112.5	GRA	0.3	Flanagan and Adkinson (2011)
ON Eastern Peatland	CAMer	m	1999–2006	45.407	75.484	WET	0.3	Roulet et al. (2007)
MN Northern Old Black Spruce	CANS1	n	1994–2006	55.880	98.481	ENF	9.1	Dunn et al. (2007)
SK Old Aspen	CAOas	a	1997–2006	53.629	106.198	DBF	21.0	Barr et al. (2007)
SK Southern Old Black Spruce	CAObs	b	2000–2006	53.987	105.112	ENF	9.4	Krishnan et al. (2008)
SK Old Jack Pine	CAOjp	j	2000–2006	53.916	104.692	ENF	16.7	Zha et al. (2009)
QC Eastern Old Black Spruce	CAQfo	q	2004–2006	49.629	74.342	ENF	13.8	Bergeron et al. (2007)
SK Harvested Jack Pine 1994	CASJ1	s	2004–2005	53.908	104.656	ENF	1.7	Zha et al. (2009)
SK Harvested jack Pine 2002	CASJ2	u	2003–2006	53.945	104.649	ENF	0.2	Zha et al. (2009)
SK Harvested Jack Pine 1975	CASJ3	v	2005–2006	53.876	104.645	ENF	5.5	Zha et al. (2009)
ON White Pine Plantation 1939	CATP4	t	2002–2007	42.710	80.357	ENF	21.0	Arain and Restrepo (2005)
AB Western Peatland	CAWP1	w	2004–2007	54.954	112.467	WET	3.0	Flanagan and Syed (2011)
OK ARM Southern Great Plains	USARM	A	2003–2007	36.606	97.489	CRO	0.5	Fischer et al. (2007)
NC Duke Forest Loblolly Pine	USDk3	D	2003–2005	35.978	79.0942	ENF	18.0	Oren et al. (2006), Stoy et al. (2006)
MA Harvard Forest	USHa1	H	1992–2006	42.538	72.1715	DBF	23.0	Urbanski et al. (2007)
ME Howland Forest	USHo1	O	1996–2004	45.204	68.7402	ENF	20.0	Richardson et al. (2009)
IL Fermi Agricultural Site	USIB1	I	2005–2007	41.859	88.2227	CRO	1.0	Post et al. (2004)
IL Fermi Prairie Site	USIB2	J	2005–2007	41.841	88.241	GRA	1.0	Post et al. (2004)
WI Lost Creek	USLos	L	2001–2006	46.083	89.9792	CSH	2.0	Sulman et al. (2009)
OR Metolius Young Ponderosa Pine Plantation	USMe3	P	2004–2005	44.315	121.608	ENF	3.1	Vickers et al. (2012b)
OR Metolius Young Ponderosa Pine Natural Regeneration	USMe5	Q	2000–2002	44.437	121.567	ENF	4.3	Law et al. (2001)
IN Morgan Monroe State Forest	USMMS	M	1999–2005	39.323	86.4131	DBF	27.0	Schmid et al. (2000)
MO Missouri Ozark Site	USMoz	Z	2005–2007	38.744	92.2	DBF	24.2	Gu et al. (2006)
NE Mead Irrigated Continuous Maize	USNe1	B	2002–2005	41.165	96.4766	CRO	2.9	Verma et al. (2005); Suyker and Verma (2010)
NE Mead Irrigated Maize-Soybean Rotation	USNe2	C	2003–2005	41.165	96.4701	CRO	1.8	Suyker and Verma (2010)
NE Mead Rainfed Maize Soybean Rotation	USNe3	E	2002–2005	41.180	96.4396	CRO	1.7	Verma et al. (2005); Suyker and Verma (2010)
CO Niwot Ridge Forest	USNR1	N	1999–2007	40.033	105.546	ENF	11.4	Monson et al. (2005)
OK Shidler Grassland	USShd	G	1998–1999	36.933	96.6833	GRA	0.6	Suyker et al. (2003)
CA Sky Oaks Old Stand	USSO2	R	2000–2002, 2006	33.377	116.623	CSL	1.0	Luo et al. (2007)
MI Sylvania Wilderness Area	USSyv	S	2002–2006	46.242	89.3477	MF	22.0	Desai et al. (2005)
CA Tonzi Ranch	USTon	T	2002–2007	38.432	120.966	WSA	9.4	Ma et al. (2007)
MI University of Michigan Biological Station	USUMB	U	1999–2006	45.560	84.7138	DBF	21.0	Nave et al. (2011)
CA Vaira Ranch	USVar	V	2001–2006	38.407	120.951	GRA	1.0	Ma et al. (2007)
WI Willow Creek	USWCr	W	2000–2006	45.806	90.0799	DBF	24.2	Cook et al. (2004)

[a] IGBP classes: CRO Cropland; CSA Closed Shrubland; DBF Deciduous Broadleaf Forest; ENF Evergreen Needleleaf Forest; GRA Grassland; MF Mixed Forest; WET Permanent Wetlands; WSA Woody Savannas.

Table 2
Percentiles of the F_{max} distribution for Eq. (1b), used to determine the significance level of detected change points. The F_{max} percentiles for 0.90, 0.95 and 0.99 correspond to significance levels of 0.10, 0.05 and 0.01, respectively.

	F_{max} percentiles		
n	$F_{max,0.90}$	$F_{max,0.95}$	$F_{max,0.99}$
10	6.299	9.147	18.266
15	5.699	7.877	13.810
20	5.517	7.443	12.648
30	5.322	7.031	11.446
50	5.303	6.876	10.664
70	5.348	6.888	10.503
100	5.447	6.918	10.453
150	5.524	6.981	10.386
200	5.614	7.062	10.560
300	5.739	7.201	10.687
500	5.873	7.342	10.675
700	6.059	7.563	11.007
1000	6.274	7.783	11.232

The respective F_c scores are, for Eq. (1a):

$$F_c = \frac{(SSE_{2a} - SSE_{1a})}{SSE_{1a}/(n - n_a)} \quad (3a)$$

and for Eq. (1b):

$$F_c = \frac{(SSE_{2b} - SSE_{1b})}{SSE_{2b}/(n - n_b)} \quad (3b)$$

where n is the number of data points (bins) and the SSE terms are the respective sum of squared errors:

$$\begin{aligned} SSE_{1a} &= \sum_{i=1}^{c}(y_i - a_0 - a_1 x_i)^2 + \sum_{i=c+1}^{n}(y_i - a_0 - a_1 x_c - a_2(x_i - x_c))^2 \\ SSE_{2a} &= \sum_{i=1}^{n}(y_i - \alpha_0 - \alpha_1 x_i)^2 \\ SSE_{1b} &= \sum_{i=1}^{c}(y_i - b_0 - b_1 x_i)^2 + \sum_{i=c+1}^{n}(y_i - b_0 - b_1 x_c)^2 \\ SSE_{2b} &= \sum_{i=1}^{n}(y_i - \beta_0)^2 \end{aligned} \quad (4)$$

To test the null hypothesis, i.e. that the data do not contain a significant change-point, model-specific critical F_{max} values are required (Lund and Reeves, 2002). For the Eq. (1a) versus Eq. (2a) comparison, the critical F_{max} given by Wang (2003) can be used. For the Eqs. (1b) versus (2b) comparison, the critical F_{max} are given in Table 2, computed for this study using the Monte-Carlo procedure described by Lund and Reeves (2002) and Wang (2003) with 100,000 repetitions.

2.4. Quality assurance

Four quality assurance criteria were applied to the u_*^{Th} estimates from Eq. (1b). Individual u_*^{Th} estimates were rejected if the change-point was not statistically significant (F test, Eq. (3a) and Table 2, 5% significance level). For each site-year, significant change-points from all strata and bootstraps were divided into modes D (deficit: $b_1 > 0$) and E (excess: $b_1 \leq 0$) based on parameter b_1 from Eq. (1b), and the u_*^{Th} estimates from the less frequent mode were eliminated. The annual analysis was rejected if the combined strata for all bootstraps contained less than 4.000 acceptable change-points or if the fraction of acceptable change-points was less than 20%. At each site, atypical years were identified and rejected based on parameters a_1 and a_2 from the diagnostic change-point model (Eq. (1a)). When a site-year passed the acceptance criteria, the acceptable u_*^{Th} values were averaged across the n_S * n_T strata within each bootstrap, producing 1.000 realizations of the annual mean. Uncertainty was determined from the distribution of the 1000 bootstraps, and is expressed either as a 95% confidence interval estimated from the 2.5 and 97.5 percentiles, or as a coefficient of variation (CV), the ratio of the standard deviation to the mean.

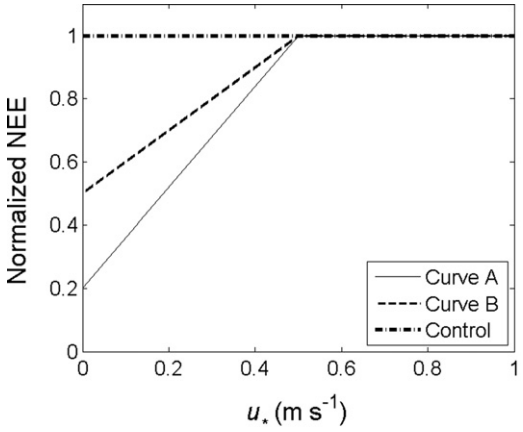

Fig. 2. Idealized (u_* versus NEE) relationships used to evaluate u_*^{Th} detection methods. The control is a flat line with no u_*^{Th}.

2.5. Diurnal, seasonal and inter-annual variation

We evaluated temporal u_*^{Th} variation at three time scales for each site. Inter-annual u_*^{Th} variation was assessed using a paired t-test of the annual values, with a separate test for each pair of years. Seasonal u_*^{Th} variation was evaluated by first computing the mean u_*^{Th} and date for each temporal moving window (across n_T temperature strata and 1000 bootstraps), then pooling the windows from all years and fitting an annual sine curve to the pooled data

$$u_*^{Th} = s_0 + s_1 \sin(\omega(d - s_2)) \quad (5)$$

where s_0 (mean), s_1 (amplitude) and s_2 (phase) are regression parameters, ω is the annual angular frequency ($2\pi/365.2425\,\text{days}^{-1}$) and d is the day of year (including decimal). The normalized annual amplitude was computed as the ratio s_1/s_0. At sites with significant seasonal u_*^{Th} variation, the u_*^{Th} was allowed to vary seasonally as estimated from Eq. (5). Nocturnal u_*^{Th} variation was assessed by estimating annual u_*^{Th} independently for five nighttime periods: the entire night; early, middle and late (each equally-sized); and dusk (identified as a 90-min period for 30-min fluxes or a 60-min period for 60-min fluxes, one period removed from sunset). To create a sufficient sample size for each nocturnal period, all years were combined prior to the analysis and the combined data were sorted by time of year.

2.6. Evaluation of threshold-detection techniques

We evaluated the original and modified u_*^{Th} detection methods using synthetic data from three idealized, normalized NEE versus u_* relationships (Fig. 2). Relationships A and B had a u_*^{Th} of 0.50 m s^{-1}, a u_* range of 0.0–1.0 m s^{-1}, but differed in the slope below the u_*^{Th}. NEE was set arbitrarily to 1.0 above the u_*^{Th}. Relationship C was a control with no change-point. Realistic, statistically-generated noise was added to NEE from a double exponential distribution (Richardson et al., 2006), with the double-exponential scale parameter β varying from 0.3 to 0.7, the number of u_* bins n_B varying between 20, 50 and 100, and the number of data points per bin n_P varying between 5 and 20. Uncertainty was estimated by repeating

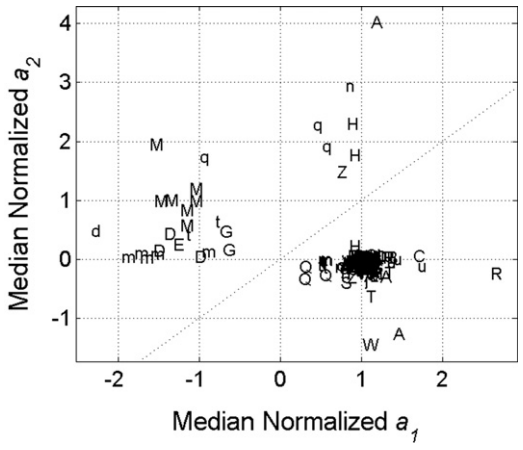

Fig. 3. Normalized parameters a_1 and a_2 from the diagnostic change-point model (Eq. (1a)), computed as annual medians from the most frequent mode (deficit or excess), and plotted annually by site code (Table 1). The values of a_1 and a_2 are normalized to an NEE value of one at $u_* = u_*^{Th}$, by multiplying each by a factor of $[u_*^{Th}/(a_0 + a_1 \cdot u_*^{Th})]$.

the process 100,000 times. The actual values of β for the site-years in this study, normalized by NEE, varied from 0.22 to 1.38, with a mean ($\pm$1 s.d.) of 0.61 ± 0.18.

2.7. Filling gaps in NEP and partitioning NEP into P and R_e

Gaps in NEP were filled using the Reichstein et al. (2005) marginal distribution sampling (MDS) filling method. Random uncertainties in NEP were estimated following Richardson et al. (2007) using synthetic data from the MDS gap-filling method (Reichstein et al., 2005). NEP was partitioned into gross primary production (P) and total ecosystem respiration (R_e) using the Barr et al. (2004) Fluxnet-Canada gap-filling/partitioning method, with slight modifications (FCM). The modifications to the Fluxnet-Canada method included: use of a weighted mean of soil and air temperature as the independent variable for estimating R_e; delineation of nighttime periods from global shortwave radiation of less than 5 W m^{-2}; and rejection of years with gaps in NEE of 31 days or longer.

3. Results

3.1. Assessing the suitability of u_*^{Th} filters

The diagnostic change-point model (Eq. (1a)) was used to assess the suitability of u_*^{Th} filters for each site-year of data (Fig. 3). Note that u_*^{Th} filters are appropriate when parameter a_1 (the NEE versus u_* slope below the change-point) is significantly different from zero and parameter a_2 (the NEE versus u_* slope above the change-point) is not significantly different from zero. The analysis (Fig. 3) produced a dense cloud of normalized (a_1, a_2) points with values near (1,0), showing NEE deficits at low u_* and uniform NEE above a well-defined u_*^{Th}. The cluster of (a_1, a_2) points near (1,0) contains 86% of the site years and includes all years from 26 of 39 sites and all but one year from 6 other sites. The points outside the cluster at (1,0) fall into two groups: sites and years with negative a_1 and near-zero a_2 where a u_*^{Th} filter is needed to resolve the problem of NEE *excesses* at low u_*; and scattered outliers where the u_*^{Th} approach does not apply. The location, dominance and tightness of the (a_1, a_2) cluster near (1,0) verifies the general need for u_*^{Th} filters to remove nighttime periods with NEE deficits at low u_*. It validates the operational use of the simplified change-point model (Eq. (1b)), which sets a_2 to zero. And it shows the usefulness of Eq. (1a) as a diagnostic tool to identify sites where the u_*^{Th} approach does not apply and years where u_*^{Th} detection fails (Table 1). Three of the six sites that had a single year with (a_1, a_2) values outside the cluster at (1,0) also had extreme u_*^{Th} estimates in that year. In our opinion, these (a_1, a_2) anomalies indicate a failure of the u_*^{Th} detection method for particular site-years so that the u_*^{Th} values from atypical years should be rejected.

3.2. Assessing u_*^{Th} methods

Before comparing the original (Papale et al., 2006) and modified u_*^{Th} methods at the study sites, we evaluated their respective threshold-detection algorithms (MPT versus CPD) using synthetic data from idealized NEE versus u_* relationships with added statistically-generated noise (Section 2.6, Fig. 2). The most striking outcomes (Table 3) are: the overall effectiveness of CPD; the serious underestimation of u_*^{Th} by MPT especially at $n_P = 5$, $n_B > 20$, and $\beta > 0.3$; the increasing rate of undetected change-points by CPD with increasing noise and decreasing n_B; and the ability of CPD to successfully detect the control case that lacks a change-point, as seen in the low (3%) acceptance rate.

Next we compared the full implementations of the two u_*^{Th} methods (original: Papale et al. (2006) versus modified: Sections 2.3 and 2.4) at the study sites (Fig. 4). The modified method produced larger and less variable u_*^{Th} estimates than the original method at 28 of 38 sites. However, the response diverged at 10 sites, all of which lacked a well-defined u_*^{Th}.

The u_*^{Th} differences between the original and modified methods were larger for synthetic than flux-tower data. The difference is in the respective implementations. The test with synthetic data evaluated the threshold-detection algorithms only (MPT versus CPD),

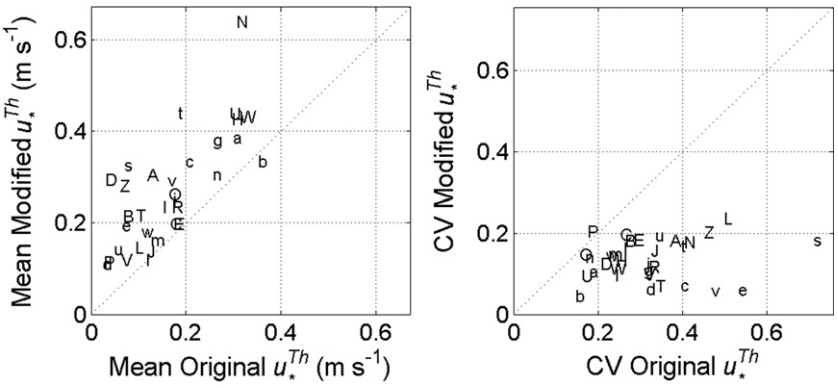

Fig. 4. Comparison of u_*^{Th} estimates from the original (Papale et al., 2006) and modified methods, by site. Left panel: annual means; right panel: mean annual coefficient of variation.

Table 3
Evaluation of two threshold-detection algorithms: moving-point test (MPT) as implemented in the original u_*^{Th} method; and change-point detection (CPD), used in the modified method. The evaluation (Section 2.6) used synthetic data from idealized curves (Fig. 2) with $u_*^{Th} = 0.50\ m\ s^{-1}$ and realistic noise added from a double exponential distribution at three levels of β. Uncertainty was estimated by performing 100,000 repetitions. The evaluation used $n_B = 20$, 50 or 100 u_* bins, each with $n_P = 5$ or 20 data points per bin. Note that the original method as implemented in Papale et al. (2006) uses $n_B = 20$ with n_P that is site dependent but generally in the order of 10–15.

				u_*^{Th} (m s^{-1}) mean ± 1 s.d. (% accepted)		
Method	Curve	n_B	n_P	$\beta = 0.3$	$\beta = 0.5$	$\beta = 0.7$
MPT	A	20	5	0.24 ± 0.09 (99%)	0.16 ± 0.07 (99)	0.13 ± 0.06 (99%)
MPT	A	20	20	0.42 ± 0.07 (100%)	0.27 ± 0.09 (100%)	0.20 ± 0.08 (100%)
MPT	A	50	5	0.05 ± 0.02 (100%)	0.04 ± 0.02 (100%)	0.03 ± 0.02 (100%)
MPT	A	100	5	0.02 ± 0.01 (100%)	0.02 ± 0.01 (100%)	0.02 ± 0.01 (100%)
MPT	B	50	5	0.04 ± 0.02 (100%)	0.03 ± 0.02 (100%)	0.03 ± 0.02 (100%)
MPT	Control	50	5	0.03 ± 0.01 (100%)	0.03 ± 0.01 (100%)	0.03 ± 0.01 (100%)
CPD	A	20	5	0.49 ± 0.13 (85%)	0.47 ± 0.16 (47%)	0.46 ± 0.17 (25%)
CPD	A	50	5	0.51 ± 0.10 (98%)	0.50 ± 0.16 (88%)	0.48 ± 0.18 (62%)
CPD	A	100	5	0.51 ± 0.07 (100%)	0.51 ± 0.13 (98%)	0.50 ± 0.17 (91%)
CPD	B	50	5	0.50 ± 0.15 (89%)	0.47 ± 0.19 (49%)	0.45 ± 0.21 (28%)
CPD	Control	50	5	0.34 ± 0.25 (3%)	0.33 ± 0.24 (3%)	0.35 ± 0.24 (3%)

whereas the comparison with flux-tower data evaluated the full implementations for annual u_*^{Th} evaluation, with three modifications to the original method: threshold-detection (MPT versus CPD); seasonal stratification (four-season versus moving-window); and aggregation (computation) of the annual value (maximum of four seasonal values versus overall mean). To isolate the relative impacts of these three changes, we implemented the changes one at a time. The results (Table 4) show large but partially offsetting impacts of the changes in threshold-detection and aggregation, and a relatively small impact of the change in stratification. Changing threshold detection alone, from MPT to CPD (Modified-T, Table 4), more than doubled the u_*^{Th} estimates, whereas changing seasonal aggregation alone, from seasonal maximum to mean (Modified-A), reduced the u_*^{Th} estimates by ~30%. The net result of the combined modifications (Modified-SAT, which is the modified method in this study) was a mean 56% increase in u_*^{Th} across all sites and years. We conclude that the original method's use of the seasonal maximum to compute the annual u_*^{Th} partially offsets the low estimates from its MPT algorithm. It is also important to note how increasing noise in the data leads to underestimation of the threshold using the MPT algorithm (Table 3 with increasing β).

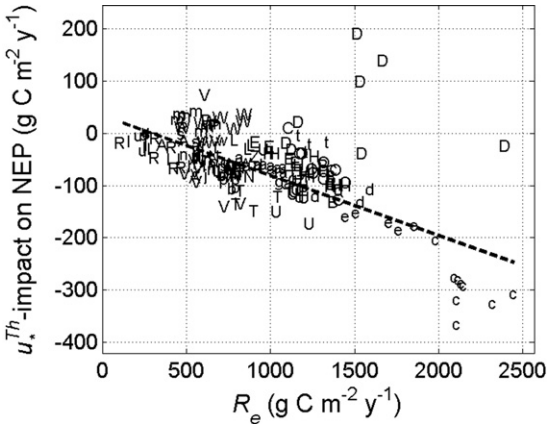

Fig. 5. Change in annual NEP (ΔNEP) caused by the application of u_*^{Th} filter, in relation to annual R_e, by site-year. ΔNEP is computed as the difference between annual NEP at the pooled median u_*^{Th} (modified method) and annual NEP calculated with no u_*^{Th} filter. Gaps in NEE were filled using the MDS method. Annual R_e was estimated using FCM gap-filling/partitioning. The linear regression relationship, applied to sites in deficit mode, is $\Delta NEP = -0.11 \cdot R_e + 34\ g\ C\ m^{-2}\ y^{-1}$ ($r^2 = 0.59$).

3.3. Impact of u_*^{Th} on NEP and R_e

Compared to no u_*^{Th} filtering, the use of the modified u_*^{Th} filter caused mean (±1 s.d.) changes of $-65 \pm 73\ g\ C\ m^{-2}\ y^{-1}$ in NEP and $+237 \pm 242\ g\ C\ m^{-2}\ y^{-1}$ in R_e across all sites and years, both of which are large compared to the overall means of 137 (NEP) and 938 (R_e) g C m^{-2} y^{-1}. The impact of the modified u_*^{Th} filter on NEP varied in relation to R_e (Fig. 5) with a positive impact for sites with NEE excesses at low u_* (e.g. CAMer ('m'), USDk3 ('D')) and a negative impact for sites with NEE deficits at low u_* (most others, where $\Delta NEP = 34 - 0.11\ R_e$, $r^2 = 0.59$).

The annual estimates for NEP and R_e were sensitive to the u_*^{Th} method (original versus modified) at some but not all sites (Fig. 6). Overall, the u_*^{Th} modifications caused a small ($-9 \pm 30\ g\ C\ m^{-2}\ y^{-1}$, mean ± 1 s.d.) reduction in NEP and a moderate ($61 \pm 111\ g\ C\ m^{-2}\ y^{-1}$) increase in R_e. However, the impact varied among sites depending on the change-point mode (deficit versus excess) and the ratio of the original to modified u_*^{Th}. At many sites, the impact was small. At 10 of 32 sites with relatively consistent u_*^{Th} behavior, however, the u_*^{Th} modifications caused a change of more than 10 g C m^{-2} y^{-1} in NEP and 10% in R_e. Notably, all ten of these sites had original to modified u_*^{Th} ratios of below 0.6. When the ratio was equal or larger than 0.7, the differences were almost zero.

To evaluate whether or not the modifications to the u_*^{Th} method altered inter-annual variability in NEP, we compared annual NEP anomalies between the modified versus original u_*^{Th} methods. At 12 of 18 sites with five years or more of data, the inter-annual NEP differences were largely unaffected by the modifications to the u_*^{Th} method. At 2 of 18 sites (CACa1 and CACa3), in contrast, the impact of the modifications was so large that the NEP

Table 4
Evaluation of the original and modified u_*^{Th}-evaluation methods at the NACP study sites, based on 191 site-years of data. Included are three partial implementations of the modified method (Section 3.2) denoted as Modified-A, Modified-T, and Modified-AT, and the complete modification denoted as Modified-SAT.

Method	Seasonal stratification	Seasonal aggregation	Threshold detection	u_*^{Th} (m s^{-1}) mean (±1 s.d.)
Original	Four-season	Maximum	MPT	0.192 ± 0.104
Modified-A	Four-season	Mean	MPT	0.137 ± 0.079
Modified-T	Four-season	Maximum	CPD	0.410 ± 0.209
Modified-AT	Four-season	Mean	CPD	0.295 ± 0.134
Modified-SAT	Seasonal moving-window	Mean	CPD	0.300 ± 0.132

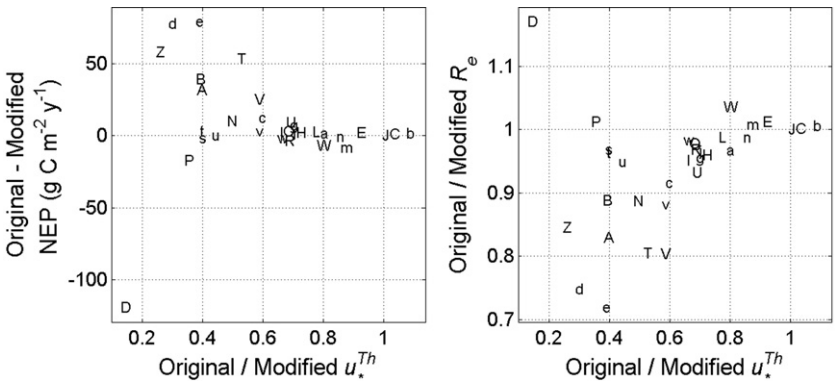

Fig. 6. Impact of modifications to the u_*^{Th}-evaluation method on mean annual NEP and R_e, by site, in relation to the ratio of the original and modified estimates of the u_*^{Th}. The left panel shows the difference between NEP estimated using the original u_*^{Th} and NEP estimated using the modified u_*^{Th}. The right panel shows the ratio of R_e estimated using the original u_*^{Th} to R_e estimated using the modified u_*^{Th}.

anomalies from the modified versus original u_*^{Th} methods were uncorrelated at the 5% significance level. At 4 others (CACa2, USNR1, USTon and USVar), the NEP anomalies from the modified versus original u_*^{Th} methods were positively correlated ($r > 0.90$, $p \leq 0.05$) but the linear-regression slopes departed by more than 20% from the one-to-one line. It may be significant that some of the sites where inter-annual variability in NEP was sensitive to the modification in the u_*^{Th} method are in locations with sloping terrain (CACa1, USNR1) or strong land-sea breeze circulations (CACa1, CACa2, CACa3).

3.4. u_*^{Th} uncertainty and the related uncertainty in NEP

The coefficient of variation for annual u_*^{Th}, as estimated by bootstrapping, had a mean (±1 s.d.) of 21% ± 10% (original method) and 8% ± 3% (modified method) across all site years, indicating tight u_*^{Th} delineation by the modified method at the annual time scale (Fig. 4). The u_*^{Th} CV was independent of plant functional type but varied by site, depending primarily on the sample size of the successful u_*^{Th} detections. Surprisingly, no relationship was observed between the annual u_*^{Th} CV and the NEE random uncertainty (computed using the approach of Richardson et al., 2007), despite large inter-site differences in the random uncertainty and the strong dependence of the u_*^{Th} CV on β in Table 3.

The sensitivity of annual NEP and R_e to uncertainty in the u_*^{Th} was computed as the difference between NEP (or R_e) at the 97.5 versus 2.5 u_*^{Th} percentiles (Fig. 7). Compared to the original method, the modified method shifted the sensitivity distribution towards a mean of zero for both fluxes, reduced the variability among site-years, and eliminated all extreme uncertainty estimates.

3.5. Temporal u_*^{Th} variation

Sections 3.5 and 3.6 report u_*^{Th} estimates from the modified method. We examined temporal variation in the u_*^{Th} over three time scales: diurnal, seasonal, and inter-annual. To investigate van Gorsel et al.'s (2007) hypothesis that periods just after dusk are free of flux measurement deficits, we evaluated the u_*^{Th} response independently for five nighttime periods using the operational

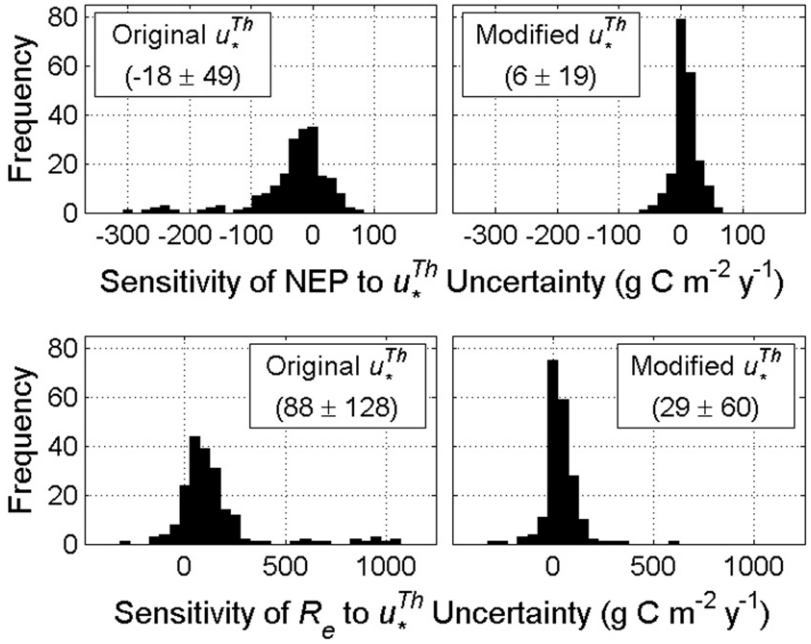

Fig. 7. Upper panels: Histograms for all site-years showing the sensitivity of annual NEP to uncertainty in the u_*^{Th}, computed as the difference between annual NEP at the 97.5 and 2.5 u_*^{Th} percentiles, for the original (left panel) and modified (right panel) u_*^{Th} methods. Gaps were filled using the MDS method. The bracketed numbers in the text boxes are the median ± inter-quartile range, in (g C m^{-2} y^{-1}). Lower panels: Same as upper panels but for annual R_e estimated using FCM gap-filling and partitioning.

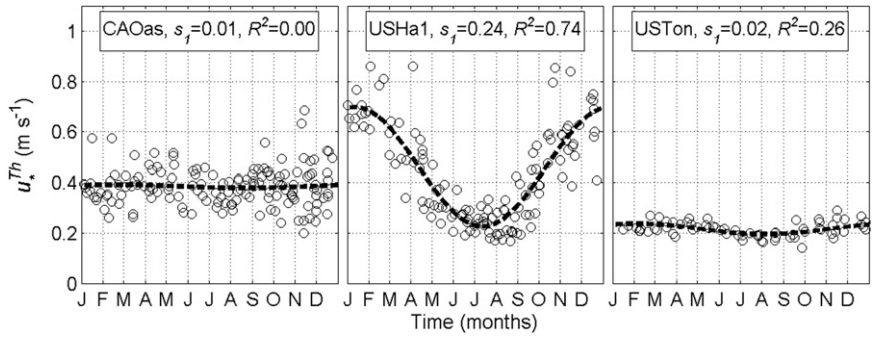

Fig. 8. Seasonal variation in the u_*^{Th} at three representative sites, estimated using temporal moving windows and with all years pooled. The dotted line is a fitted annual sine curve (Eq. (5)) with amplitude s_1 and coefficient of determination R^2.

change-point model (Eq. (1b)). The analysis showed no significant time-of-night differences in u_*^{Th}, parameters b_0 and b_1, or the fitted NEP asymptote (i.e. $b_0 + b_1\ u_*^{Th}$), indicating the occurrence of similar NEP flux deficits at low u_* throughout the night.

Figs. 8 and 9 address the questions: Does the u_*^{Th} vary seasonally? And what is the impact on annual NEP? The analysis showed consistent seasonal u_*^{Th} variation at some sites. Fig. 8 gives examples of three contrasting u_*^{Th} annual cycles: unvarying (near-zero s_1/s_0 and near-zero R^2, Eq. (5)) (CAOas); variable with consistent phase and large amplitude (high s_1/s_0 and high R^2) (USHa1); and variable with consistent phase and small amplitude (low s_1/s_0 and moderate R^2) (USTon). The s_1/s_0 ratio varied among sites from 0.02 to 0.51 (median 0.13). At many sites including all sites with s_1/s_0 ratios above 0.30, the phase and amplitude of the u_*^{Th} annual cycle were consistent among years, and the u_*^{Th} annual cycle was in phase with the nighttime-u_* annual cycle. Inter-site differences in the u_*^{Th} annual amplitude (s_1) were positively related to the nighttime u_* annual amplitude ($r^2 = 0.60$) and mean annual nighttime u_* ($r^2 = 0.56$). However, applying a seasonally-varying u_*^{Th} filter had little impact on NEP (compared to NEP estimated using the annual mean u_*^{Th}) except for the two sites with the greatest variation in annual u_*^{Th} (Fig. 9). At these sites, the use of a seasonally-varying u_*^{Th} filter altered NEP by -34 ± 14 g C m^{-2} y^{-1} (USHa1) and -41 ± 13 g C m^{-2} y^{-1} (USWCr).

We found that u_*^{Th} at a site varies only slightly among years, and that the impact of this variation on annual NEP is small. A paired t-test applied to all pairs of years at each site showed significant inter-annual differences in the u_*^{Th} for 96% of the paired years. Despite the statistical significance of the inter-annual u_*^{Th} differences, however, the inter-annual CV of the mean annual u_*^{Th} was small (mean 11%), similar to the mean intra-annual (among-bootstrap) u_*^{Th} CV of 8%. When all years were pooled within each site, the mean CV of the pooled u_*^{Th} increased only slightly, from 8% (within-year) to 14% (pooled). We have not identified a physical basis for inter-annual differences in the u_*^{Th} except for sites where the physical characteristics change among years, such as in a young, rapidly-growing forest. For that reason, and because the u_*^{Th} analysis may be compromised by undetected data problems during some years, we recommend the pooling of u_*^{Th} estimates from all years after problem years are excluded. Pooling increases the u_*^{Th} uncertainties a little, but prevents the use of anomalous u_*^{Th} values from years where large data gaps or unidentified data problems have weakened the u_*^{Th} analysis. In addition, pooling enables the use of consistent u_*^{Th} values for all years, thus avoiding the potential introduction of NEP extremes for years with unreliable u_*^{Th} values.

The pooling of annual u_*^{Th} estimates among years, rather than the use of annual u_*^{Th} estimates, had only a small impact on NEP. The mean (± 1 s.d.) difference in NEP between pooled and annual u_*^{Th} values was 0 ± 5 g C m^{-2} y^{-1} across site years, with an increase in the (mean $\pm$ 1 s.d.) u_*^{Th}-related 95% confidence interval in NEP from 6 ± 5 (annual) to 9 ± 6 (pooled) g C m^{-2} y^{-1}. These differences are surprisingly small when compared to the overall NEP mean of 137 g C m^{-2} y^{-1}. They demonstrate the robustness of CPD and the consistency of the u_*^{Th} values among years. In addition, inter-annual variability in NEP was not significantly impacted by the pooling of annual u_*^{Th} estimates among years at any of the 18 sites with five or more years of data.

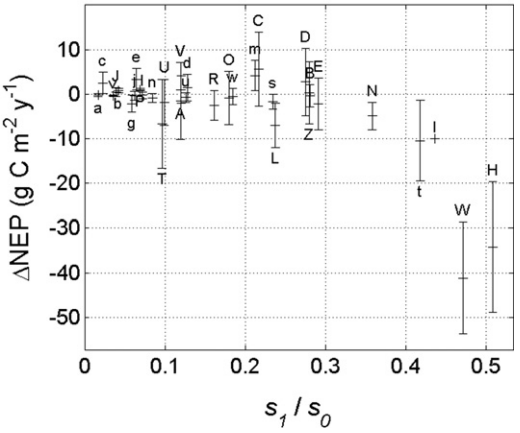

Fig. 9. Impact of seasonal variation in the u_*^{Th} on annual NEP (computed as the difference between annual NEP using a seasonally-varying u_*^{Th} filter and annual NEP at the median annual u_*^{Th}), as a function of the s_1/s_0 ratio from Eq. (5). Gaps in NEP were filled using the MDS method. The error bars show one s.d. from the mean.

3.6. u_*^{Th} variation among sites

The u_*^{Th} varied by site (Table 5) and in relation to plant functional type (Table 6). The sites in this study divide naturally into three groups: non-forested lands, including grasslands, croplands and wetlands, with mean h_c of 1.8 m and mean (± 1 s.d.) u_*^{Th} of 0.20 ± 0.06 m s^{-1}; juvenile forests with mean h_c of 4.1 m and u_*^{Th} of 0.24 ± 0.10 m s^{-1}; and mature forests with mean h_c of 20 m and u_*^{Th} of 0.38 ± 0.10 m s^{-1}. The u_*^{Th} is strongly, positively related to mean annual nighttime u_* (Fig. 10 left panel, $r^2 = 0.81$) and positively related to canopy height (Fig. 10 right panel, $r^2 = 0.42$).

Of the 38 sites in this study, 10 sites showed significant deviations from the expected u_*^{Th} deficit response (Table 5). One site (USDk3) had well-defined u_* values but with NEE excesses rather than deficits at low u_*; see Oren et al. (2006) for a detailed discussion of the measurement issues at this site, which is situated in a heterogeneous landscape (30 ha pine plantation adjacent to grassland, deciduous forest, and suburban development). At 9 other sites, the u_*^{Th} algorithm was unable to identify a clear, consistent u_*^{Th}. The lack of clarity was evidenced by: a high failure rate in u_*^{Th} detection (CAMer, CAQfo, CATP4, USMMS, USMe5, USNe3, USShd);

Table 5
Parameters from the u_*^{Th} analysis.

Site code	u_*^{Th} mean (CI) (m s^{-1})	s_1 (r^2) (Eq. (5))	Mode	% Deficit	% Select
CACa1	0.33 (0.05)	0.01 (0.01)	Deficit	100	98
CACa2	0.12 (0.03)	0.01 (0.32)	Deficit	100	94
CACa3	0.19 (0.02)	0.01 (0.10)	Deficit	100	97
CAGro	0.38 (0.08)	0.02 (0.03)	Deficit	100	65
CALet	0.23 (0.05)	0.02 (0.06)	Deficit	100	95
CAMer	0.16 (0.05)	0.03 (0.20)	Mixed	47	42
CANS1	0.32 (0.10)	0.03 (0.06)	Deficit	100	70
CAOas	0.39 (0.08)	0.01 (0.00)	Deficit	100	89
CAObs	0.33 (0.03)	0.01 (0.04)	Deficit	100	99
CAOjp	0.25 (0.06)	0.02 (0.03)	Deficit	100	83
CAQfo	0.29 (0.13)		Deficit	100	17
CASJ1	0.33 (0.11)	0.08 (0.15)	Deficit	99	50
CASJ2	0.14 (0.05)	0.02 (0.06)	Deficit	100	63
CASJ3	0.29 (0.03)	0.01 (0.02)	Deficit	100	84
CATP4	0.50 (0.38)	0.20 (0.61)	Deficit	96	42
CAWP1	0.18 (0.05)	0.03 (0.16)	Deficit	99	77
USARM	0.33 (0.11)	0.04 (0.09)	Deficit	100	48
USDk3	0.29 (0.07)	0.08 (0.45)	Excess	0	87
USHa1	0.42 (0.11)	0.23 (0.75)	Deficit	100	62
USHo1	0.26 (0.07)	0.05 (0.27)	Deficit	100	94
USIB1	0.12 (0.04)	0.07 (0.38)	Deficit	100	46
USIB2	0.14 (0.04)	0.01 (0.01)	Deficit	100	73
USLos	0.15 (0.06)	0.04 (0.20)	Deficit	100	75
USMe3	0.11 (0.05)	0.01 (0.04)	Deficit	85	47
USMe5	0.33 (0.13)		Mixed	51	24
USMMS	0.49 (0.18)		Mixed	37	29
USMoz	0.29 (0.10)	0.08 (0.25)	Deficit	98	48
USNe1	0.21 (0.07)	0.07 (0.34)	Deficit	100	52
USNe2	0.20 (0.07)	0.04 (0.26)	Deficit	100	49
USNe3	0.23 (0.09)	0.06 (0.40)	Deficit	100	32
USNR1	0.64 (0.20)	0.23 (0.49)	Deficit	100	88
USShd	0.25 (0.05)		Deficit	80	30
USSO2	0.23 (0.05)	0.04 (0.17)	Deficit	100	56
USSyv	0.37 (0.08)		Deficit	90	39
USTon	0.22 (0.03)	0.02 (0.26)	Deficit	100	87
USUMB	0.44 (0.08)	0.04 (0.21)	Deficit	100	93
USVar	0.12 (0.02)	0.01 (0.22)	Deficit	100	69
USWCr	0.40 (0.16)	0.18 (0.64)	Deficit	100	79

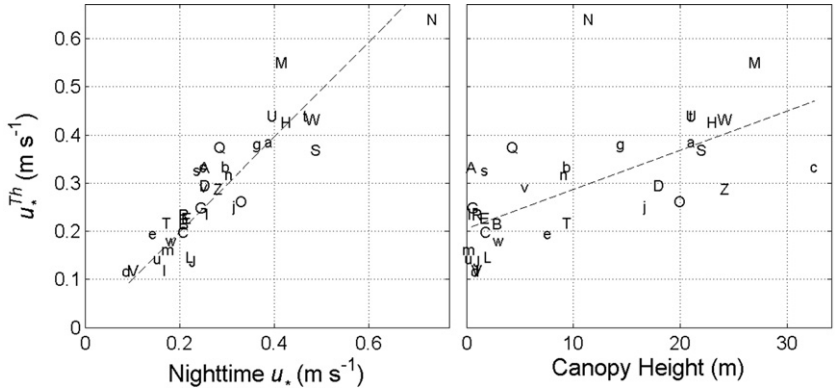

Fig. 10. Dependence of mean annual u_*^{Th} on mean annual nighttime u_* (left panel) and canopy height (right panel) across all sites. The linear regression fits are: $u_*^{Th} = 0.988\ u_*$, $r^2 = 0.79$ (forced through origin, y intercept not significantly different from zero), and $u_*^{Th} = 0.205\ \text{m s}^{-1} + 0.0081\ h_c$ (h_c in m) ($r^2 = 0.42$).

Table 6
Variation in u_*^{Th} by plant functional type. n is the number of sites for each plant functional type, h_c is the canopy height, and the values of h_c and u_*^{Th} are the mean and (s.d).

Plant functional type	n	h_c (m)	u_*^{Th} (m s^{-1})
Grasslands	4	0.7 (0.3)	0.18 (0.07)
Permanent wetlands	2	1.1 (1.6)	0.17 (0.01)
Croplands	5	1.6 (0.9)	0.22 (0.08)
Juvenile forests	6	3.3 (2.7)	0.24 (0.10)
Shrublands, savannas	3	4.1 (4.6)	0.20 (0.05)
Evergreen needleleaf forests	8	18.1 (8.2)	0.36 (0.13)
Mixedwood forests	2	19.9 (4.6)	0.37 (0.01)
Deciduous broadleaf forests	6	23.4 (2.3)	0.42 (0.09)

non-zero values of the NEE versus u_* slope above the u_*^{Th} (parameter a_2, Eq. (1a)) (CAQfo, USARM, USMMS); and the presence of mixed deficit and excess modes (CAMer, CATP4, USARM, USMe5, USNe3, USShd). At one site, the lack of clarity was explained by previously-unresolved data quality issues, as confirmed by the site investigators; the u_*^{Th} analysis succeeded when the quality issues were resolved. At other sites, however, the lack of a consistent u_*^{Th} response remains unexplained. We were not able to identify site characteristics that differentiated sites where the u_*^{Th} concept was appropriate from sites where it was not. We do not know if the cause is micrometeorological, based on site characteristics, or

technical, based on the EC and data processing system design. It is possible that the u_*^{Th} concept is not universally applicable.

4. Discussion

4.1. Appropriateness of u_*^{Th} filters

The diagnostic change-point model confirmed the suitability, robustness and clarity of u_*^{Th} filters at most flux-tower sites. At the majority of sites in this study, the u_*^{Th} was well defined, had low uncertainty, and was reasonably consistent among years. A few sites had a single year where the u_*^{Th} analysis was atypical, which we attributed to unidentified data problems. A few others lacked a clear, stable u_*^{Th} response. Because some sites and years did not follow the classic u_*^{Th} response, we recommend that the u_*^{Th} analysis be carefully scrutinized for each site-year of data before the u_*^{Th} approach is applied.

Alternatives to u_*^{Th} filters fall into two classes: advection estimation and other screening techniques. Many studies have attempted to resolve the problem of nighttime NEE measurement deficits by including terms for horizontal and vertical advection in the flux calculations (e.g., Feigenwinter et al., 2004, 2008; Staebler and Fitzjarrald, 2004; Marcolla et al., 2005; Aubinet et al., 2005, 2010; Heinesch et al., 2008; Leuning et al., 2008; Montagnani et al., 2009). The direct measurement of advection is theoretically attractive; however, it is becoming increasingly clear that the routine measurement of advection may not be feasible because of the enormous data requirements (Aubinet et al., 2010; Canepa et al., 2010). In the most intensive field study of advection to date, conducted in three European forests, Aubinet et al. (2010) concluded that the advection estimates were too uncertain to assess CO_2 budget closure; their order of magnitude was unreasonable and the resulting fluxes varied with wind direction and u_* in a non-biological way. The very large uncertainties associated with measuring horizontal and vertical advection make it impractical to include advection in the routine computation of turbulent fluxes (Aubinet et al., 2003; Feigenwinter et al., 2008; Leuning et al., 2008). They highlight the need to further evaluate and improve alternate solutions to the nighttime flux deficit problem, including u_*^{Th} filtering.

Alternate screening techniques include: filtering with the vertical velocity standard deviation (σ_w) (Black et al., 1996; Acevedo et al., 2009) or buoyancy forcing fraction (Staebler and Fitzjarrald, 2004), and evaluating nighttime NEE based on the NEE maximum that occurs soon after sunset (van Gorsel et al., 2007, 2008, 2009). Black et al. (1996) found that a σ_w threshold filter outperformed u_*^{Th} above the understory at CAOas. A u_*^{Th} filter was better above the stand. Acevedo et al. (2009) analyzed the performance of σ_w and u_* at three contrasting sites. They concluded that σ_w is more suitable than u_* for screening NEE deficit periods because it depends on local turbulence alone whereas u_* is also affected by mesoscale motions. We would add that σ_w is a simpler measurement than u_* and thus less prone to error. A more extensive comparison of σ_w and u_* filters across many sites is needed. One practical advantage of u_*^{Th} over σ_w filters is that u_* is widely available in most national and international flux-tower databases whereas σ_w is not. Our expectation is that σ_w and u_*^{Th} filters will perform similarly; above-canopy σ_w and u_* can both become decoupled from turbulence in the lower canopy under strongly stable conditions (Launiainen et al., 2007; Nemitz et al., 2009; van Gorsel et al., 2011). Improved filters may require the addition of in-canopy turbulence measurements.

Staebler and Fitzjarrald (2004) developed a more physically-based screening variable, the buoyancy forcing fraction, that outperformed u_*^{Th} at the Harvard forest. Relative to u_*^{Th} of 0.20 m s^{-1}, the buoyancy forcing fraction increased the estimated frequency of deficit nights from 41% to 58%, thus increasing the impact of data screening. However, the buoyancy forcing fraction requires spatially extensive measurements of near surface temperature and humidity that are not routinely available at most sites. Moreover, our estimate of the u_*^{Th} at the Harvard forest is higher than 0.20 m s^{-1}, ranging from 0.23 to 0.63 m s^{-1} during the Staebler and Fitzjarrald (2004) analysis periods, which increases the estimated frequency of nighttime deficit periods to 60%, comparable with Staebler and Fitzjarrald's (2004) estimate of 58%.

van Gorsel et al. (2007, 2008) proposed a novel alternative to u_*^{Th} filters based on the observation that the NEE daily cycle reaches a maximum soon after dusk. They hypothesized that the period just after dusk is free of NEE flux deficits; nighttime flux deficits do not occur until well after dusk, when atmospheric stratification has become strongly stable and stationary mesoscale circulations and drainage flows are established. After data screening (to eliminate outliers, periods with very stable atmospheric stability or rain, and nights with highly variable NEE), the van Gorsel method computes the NEE maximum from the 3-h period after dusk, and then fills gaps using empirical relationships fitted to the daily post-dusk NEE maxima. Their approach showed good agreement with chamber-based estimates of nighttime NEE, whereas u_*^{Th}-based estimates were systematically low compared to the chambers (van Gorsel et al., 2009). Further evaluation of the van Gorsel method is warranted, including a comparison with the CPD-u_*^{Th} method from this study. Two issues merit further attention: the possibility that the van Gorsel method introduces a positive bias in nighttime NEE through the selection of the post-dusk NEE maximum from a three-hour window rather than an independent, objective identification of the optimal period; and the observation from this study that similar NEE flux deficits at low u_* occur throughout the night. Although many of the sites in this study showed an NEE maximum soon after dusk, the lower NEE values later in the night were related to: declining wind speeds, which increased the number of deficit periods; and declining temperature.

We conclude that u_*^{Th} filters should continue to be used operationally until more definitive methods are found. Where possible, they should be used in consort with other approaches. Despite their physical simplicity, u_*^{Th} filters provide a pragmatic solution to a serious problem. Their modest data requirements make them universally applicable, even with existing historic databases. The modified u_*^{Th} implementation from this study improves upon earlier implementations, producing robust u_*^{Th} estimates at most sites, eliminating a low bias, reducing the u_*^{Th}-related uncertainties in annual NEP, R_e and P, and identifying sites and site-years where the u_*^{Th} approach should not be applied.

4.2. Relation of u_*^{Th} to site characteristics

The sites in this study fell into three categories. Most (~70% of sites) had flux deficits at low u_* with a well-defined u_*^{Th}; one or two had flux excesses at low u_*; and a few (~25% of sites) lacked a clear and consistent u_*^{Th}. However, we were not able to identify site characteristics that enabled us to determine *a priori* whether the u_*^{Th} approach was suited to particular sites. A more detailed investigation is warranted, relating the u_*^{Th} behavior to, e.g., local and regional topography as well as spatial heterogeneity in land cover.

For sites with a well-defined u_*^{Th}, the u_*^{Th} was strongly dependent on u_*, both among sites ($r = 0.90$, where r is the correlation coefficient between annual u_*^{Th} and mean annual nighttime u_*), and among seasons at sites with a pronounced seasonal u_*^{Th} cycle, e.g. USHa1 and USNR1 ($r = 0.85$ and 0.49 respectively, where r is the correlation coefficient between seasonally-varying values of u_*^{Th} and nighttime u_* at the site). We have not found a hypothesis to explain both of these dependencies in consort. The among-site relationship between u_*^{Th} and u_* may result from the effect of

canopy height on the in-canopy attenuation of shear-generated turbulence, and the positive correlation between above-canopy u_* and canopy height ($r = 0.61$). Compared to croplands, forest canopies have lower σ_w/u_* ratios near the ground (Finnigan, 2000) and thus require higher above-canopy u_* or σ_w values to sustain mechanical mixing in the lower canopy and prevent the development of intermittent turbulence or advective transport. Another possibility that would artificially strengthen the among-site relationship between u_*^{Th} and u_* is that u_* is not calculated uniformly, with inter-site differences in, e.g., the choice of the u_* equation, the coordinate rotation scheme, or the care and frequency of instrument leveling. More perplexing than the among-site dependence of u_*^{Th} on mean annual nighttime u_*, however, is the seasonal dependence of u_*^{Th} on u_* at sites with seasonal u_* cycles. Further analysis is needed to identify a physical mechanism, relating the seasonal variation in u_*^{Th} to, e.g., seasonal changes in site characteristics (leaf area index, aerodynamic roughness, snow cover, energy fluxes) or the synoptic wind regime (speed and direction) and its interaction with local topography.

4.3. Comparison with other u_*^{Th} approaches

The u_*^{Th} values from this study's modified method are higher than previous estimates. Section 3.2 identified a low bias in the MPT algorithm of the original method (Papale et al., 2006). We believe that the MPT algorithm of Gu et al. (2005), which is conceptually similar to the original method, may be subject to a similar low bias. At the four sites that these studies share in common (CAOas, USHa1, USTon and USVar), Gu et al. (2005) reported June-August u_*^{Th} values of 0.02, 0.08, 0.11 and 0.00 m s^{-1} respectively, compared to this study's estimates of 0.25, 0.14, 0.06 and 0.02 m s^{-1} (original method) and 0.38, 0.26, 0.19 and 0.12 m s^{-1} (modified method). These differences are large and illustrate the difficulty of developing and implementing a robust algorithm for u_*^{Th} evaluation. They also confirm that u_*^{Th} evaluation is one of the most if not the most important source of uncertainty in EC data.

The relatively high u_*^{Th} values from this study's modified method partially resolve the criticism that u_*^{Th} filters under-correct nighttime flux deficits, resulting in a high bias in NEP and a low bias in R_e and P (van Gorsel et al., 2009; Yi et al., 2008). Relative to the original method, the higher u_*^{Th} estimates from the modified method in this study reduced NEP and increased R_e and P at most sites while reducing the u_*^{Th}-related uncertainties in all three fluxes. If eddy-covariance estimates of R_e and P are indeed routinely biased low, this increase is a step in the right direction, albeit a small one; the overall mean (± 1 s.d.) increase in R_e between the original and modified u_*^{Th} method was 62 ± 112 g C m^{-2} y^{-1} or about 7%. Our results highlight the importance of proper implementation of u_*^{Th} evaluation to minimize potential systematic errors in NEP, R_e and P caused by a low bias in the u_*^{Th}.

The u_*^{Th} had a large impact on annual NEP, R_e and P at most sites, however, the u_*^{Th}-related uncertainty in these fluxes, estimated through bootstrapping, was small. This welcome result confirms the robust nature of the modified u_*^{Th} method. Previous reports of larger u_*^{Th}-related uncertainties in NEP (Papale et al., 2006) are related to an underestimation of u_*^{Th} that caused the bootstrapped u_*^{Th} estimates to span a range where NEE was sensitive to u_*. The u_*^{Th}-related uncertainties in NEP from this study (mean 95% confidence interval of 9 g C m^{-2} y^{-1}) were much smaller than the u_*^{Th} impact on annual NEP (mean -65 g C m^{-2} y^{-1}) and the NEP random uncertainty (mean 95% confidence interval of 29 g C m^{-2} y^{-1}, computed following Richardson et al., 2007). We conclude that, although the u_*^{Th} impact on NEP is large, especially at sites with high R_e, change-point detection methods find a rather distinct u_*^{Th} at many sites, with associated NEP uncertainty estimates that are smaller than those produced by other u_*^{Th}-evaluation methods.

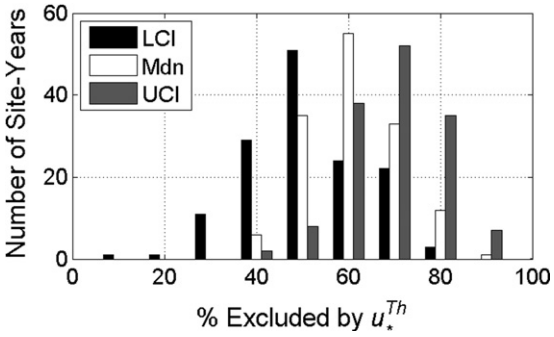

Fig. 11. Histogram of fractional data exclusion at the lower u_*^{Th} 95% confidence interval (LCI), median u_*^{Th} (Mdn), and upper u_*^{Th} 95% confidence interval (UCI), as estimated by bootstrapping, for all site years.

4.4. Impact of nighttime data exclusion

The high u_*^{Th} values resulted in a high fraction of nighttime NEE measurements that must be excluded. Across all site-years, the exclusion fraction ranged from 37% to 87% ($61\% \pm 10\%$, mean ± 1 s.d.) at the median u_*^{Th}, increasing to $70\% \pm 9\%$ at the u_*^{Th} upper 95% confidence limit (Fig. 11). The high exclusion fraction begs the question: How much data exclusion is possible without negatively affecting the gap-filling analysis? To address this question, we introduced artificial gaps into realistic synthetic NEE time series and then filled the gaps using the MDS and FCM methods. The synthetic data were created for each site year using the model output of the gap-filling models, tuned to the measured data, with added random noise based on a random uncertainty analysis (Richardson et al., 2007). Uncertainty was estimated by bootstrapping (1000 times). The analysis showed the gap-filling methods to be remarkably robust. Fractional nighttime data exclusions of 20%, 40%, 60%, 80%, and 90% applied to all site years caused mean changes in MDS NEP of 0.5, 1, 2, 4 and 8 g C m^{-2} y^{-1}, respectively (relative to the overall mean NEP of 137 g C m^{-2} y^{-1}), and mean increases in the NEP 95% confidence intervals of 1, 2, 4, 9 and 14 g C m^{-2} y^{-1}, respectively (relative to the overall mean confidence interval of 18 g C m^{-2} y^{-1}). Even with extreme (90%) fractional data exclusion, the impact on NEP was small compared to the alternate option of underestimating the u_*^{Th}. We conclude that the relatively high u_*^{Th} estimates from this study, with their high fractional data exclusions, did not compromise the annual analysis and were needed to resolve the problem of nighttime measurement deficits.

5. Summary and conclusions

This study revisited the use of u_*^{Th} filters for nighttime NEE data exclusion at 38 AmeriFlux and Fluxnet-Canada sites used in the NACP site-level syntheses. Automated u_*^{Th} assessment was improved through the incorporation of established methods for change-point detection. Compared to the original method (Papale et al., 2006) which used a moving-point test, the modified method with change-point detection produced higher u_*^{Th} estimates with lower uncertainty and was able to identify sites and years that lacked a u_*^{Th} response. The modifications increased mean annual u_*^{Th} across all site-years by 56% but decreased the mean coefficient of variation of annual u_*^{Th}, estimated by bootstrapping, from 21% to 8%. In addition, the modified method included statistical tests to identify sites that lacked a well-behaved u_*^{Th} response – 9 of the 38 sites in this study.

Compared with the original method, the higher u_*^{Th} estimates from the modified method produced a small (-9 ± 30 g C m^{-2} y^{-1}, mean $\pm$ 1 s.d.) reduction in annual NEP across all site-years, and a moderate (62 ± 112 g C m^{-2} y^{-1}) increase in R_e, compared to the overall means of 137 (NEP) and 938 (R_e) g C m^{-2} y^{-1}. More importantly, they stabilized the annual NEP and R_e estimates, reducing the mean 95% confidence intervals from 24 to 9 g C m^{-2} y^{-1} (NEP) and 82 to 39 g C m^{-2} y^{-1} (R_e). These u_*^{Th}-related uncertainties were small when compared to the mean NEP random uncertainties of 29 g C m^{-2} y^{-1}. Although the higher u_*^{Th} values from the modified method resulted in a high fractional exclusion of nighttime NEE data (61% $\pm$ 10% at the median u_*^{Th}, mean $\pm$ 1 s.d.), the negative impact of high fractional data exclusion on annual, gap-filled NEP was small compared to the more serious impact of underestimating the u_*^{Th}.

The use of a single u_*^{Th} value was warranted at most sites. Inter-annual variation in the u_*^{Th}, although significant, was small, and the pooling of annual u_*^{Th} estimates among years minimized the impact of years with spurious u_*^{Th} values. No variation in the u_*^{Th} was observed by time of day (dusk versus mid or late night), but a few sites showed significant u_*^{Th} variation with time of year. The use of a seasonally varying u_*^{Th} had a significant impact on NEP at only 2 of 38 sites. Among site-variation in the u_*^{Th} was related to site characteristics, in particular to the mean annual nighttime u_* and the canopy height.

Although the use of u_*^{Th} filters is pragmatic, based on a simple analysis of a complex problem, this study produced results at most sites that were robust, repeatable and comparable among years. We therefore recommend the continued use of u_*^{Th} filters, with three operational suggestions:

1. A diagnostic change-point model such as Eq. (1a) should be run annually to confirm that u_*^{Th} filtering is appropriate, i.e. that the analysis consistently produces statistically significant change-points with parameter a_1 that is consistently different from zero and parameter a_2 that is not consistently different from zero.
2. For sites that pass the diagnostic test, an operational change-point model such as Eq. (1b) should be run annually, with bootstrapping to estimate uncertainty. The results should be scrutinized using quality-assurance procedures such as Section 2.4. The quality assurance must allow for the detection of failure, flagging problematic or spurious years at sites that normally have a well-defined u_*^{Th}.
3. After problematic or spurious years have been excluded, the annual u_*^{Th} estimates from all bootstraps should be pooled across years, producing a u_*^{Th} distribution that can be used to identify a site-specific u_*^{Th} (the median) and to estimate the u_*^{Th}-related uncertainty in annual NEP (by estimating NEP across the u_*^{Th} distribution).

Progress towards a more fundamental yet widely-applicable alternative to u_*^{Th} filters is expected to be slow. However, we urge that u_*^{Th} filters not be considered a substitute for the development of more physically-based solutions. Progress will be hastened by the increasing availability of independent estimates of NEP, R_e and P from biometric and chamber studies (Law et al., 1999; van Gorsel et al., 2009; Vickers et al., 2012a).

Acknowledgements

We thank the NACP Site Synthesis and the Ameriflux and Fluxnet-Canada/Canadian Carbon Program investigators who provided the data on which this analysis is based. We thank the NACP Site Synthesis for support to all investigators to travel to a series of workshops that fostered this research. We also thank the funding agencies that have supported these long-term, flux-tower networks. AGB acknowledges support from the Climate Research Division of Environment Canada and thanks Xiaolin Wang for advice on change-point detection techniques and two anonymous reviewers for their constructive comments. ADR and DYH acknowledge support from Office of Science (BER), US Department of Energy, through the Terrestrial Carbon Program under Interagency Agreement No. DE-AI02-07ER64355 and through the Northeastern Regional Center of the National Institute for Climatic Change Research. DP thanks the GHG-Europe and CarboExtreme European Research projects for their support. Effort by MLF and collection of US-ARM site data were supported at LBNL by the U.S. Department of Energy, Office of Biological and Environmental Research, under contract number DE-AC02-05CH1123.

References

Acevedo, O.C., Moraes, O.L.L., Degrazia, G.A., Fitzjarrald, D., Manzi, A.O., Campos, J.G., 2009. Is friction velocity the most appropriate scale for correction of nocturnal carbon dioxide fluxes? Agric. For. Meteorol. 149, 1–10.

Amiro, B.D., Barr, A.G., Barr, J.G., Black, T.A., Bracho, R., Brown, M., Chen, J., Clark, K.L., Davis, K.J., Desai, A.R., Dore, S., Engel, V., Fuentes, J.D., Goulden, M.L., Kolb, T.E., Lavigne, M.B., Law, B.E., Margolis, H.M., Martin, T., McCaughey, J.H., Montes-Helu, M., Noormets, A., Randerson, J.T., Starr, G., Xiao, J., 2010. Ecosystem carbon dioxide fluxes after disturbance in forests of North America. JGR-Biogeosciences 115, G00K02, http://dx.doi.org/10.1029/2010JG001390.

Anderson, D.E., Verma, S.B., Rosenberg, N.J., 1984. Eddy correlation measurements of CO_2: latent heat and sensible heat fluxes over a crop surface. Agric. For. Meteorol. 29, 263–272.

Arain, M.A., Restrepo, N., 2005. Net ecosystem production in an eastern white pine plantation in southern Canada. Agric. For. Meteorol. 128, 223–241.

Aubinet, M., Grelle, A., Ibrom, A., Rannik, U., Moncrieff, J., Foken, T., Kowalski, A.S., Martin, P.H., Berbigier, P., Bernhofer, Ch., Clement, R., Elbers, J., Granier, A., Grunwald, T., Morgenstern, K., Pilegaard, K., Rebmann, C., Snijders, W., Valentini, R., Vesala, T., 2000. Estimates of the annual net carbon and water exchange of forests: the EUROFLUX methodology. Adv. Ecol. Res. 30, 113–175.

Aubinet, M., Heinesch, B., Yernaux, M., 2003. Horizontal and vertical CO_2 advection in a sloping forest. Boundary-Layer Meteorol. 108, 397–417.

Aubinet, M., Berbigier, P., Bernhofer, C., Cescatti, A., Feigenwinter, C., Granier, A., Grunwald, T., Havrankova, K., Heinesch, B., Longdoz, B., Marcolla, B., Montagnani, L., Sedlak, P., 2005. Comparing CO_2 storage and advection conditions at night at different CARBOEUROFLUX sites. Boundary-Layer Meteorol. 116, 63–93.

Aubinet, M., 2008. Eddy covariance CO_2 flux measurements in nocturnal conditions and analysis of the problem. Ecol. Appl. 18 (1), 1368–1378.

Aubinet, M., Feigenwinter, C., Heinesch, B., Bernhofer, C., Canepa, E., Lindroth, A., Montagnani, L., Rebmann, C., Sedlak, P., Van Gorsel, E., 2010. Direct advection measurements do not help to solve the nighttime CO_2 closure problem – evidence from three inherently different forests. Agric. For. Meteorol. 150, 655–664.

Baldocchi, D., Falge, E., Gu, L.H., Olson, R., Hollinger, D., Running, S., Anthoni, P., Bernhofer, C., Davis, K., Evans, R., Fuentes, J., Goldstein, A., Katul, G., Law, B., Lee, X.H., Malhi, Y., Meyers, T., Munger, W., Oechel, W., Paw, U.K.T., Pilegaard, K., Schmid, H.P., Valentini, R., Verma, S., Vesala, T., Wilson, K., Wofsy, S., 2001. FLUXNET: A new tool to study the temporal and spatial variability of ecosystem-scale carbon dioxide, water vapor, and energy flux densities. Bull. Am. Meteorol. Soc. 2, 2415–2434.

Baldocchi, D., 2008. Breathing of the terrestrial biosphere: lessons learned from a global network of carbon dioxide flux measurement systems. Aust. J. Bot. 56, 1–26.

Barford, C.C., Wofsy, S.C., Goulden, M.L., Munger, J.W., Pyle, E.H., Urbanski, S.P., Hutyra, L., Saleska, S.R., Fitzjarrald, D., Moore, K., 2001. Factors controlling long- and short-term sequestration of atmospheric CO_2 in a mid-latitude forest. Science 294, 1688–1691, http://dx.doi.org/10.1126/science.1062962.

Barr, A.G., Black, T.A., Hogg, E.H., Kljun, N., Morgenstern, K., Nesic, Z., 2004. Inter-annual variability in the leaf area index of a boreal aspen-hazelnut forest in relation to net ecosystem production. Agric. For. Meteorol. 126, 237–255.

Barr, A.G., Morgenstern, K., Black, T.A., McCaughey, J.H., Nesic, Z., 2006. Surface energy balance closure by the eddy-covariance method above three boreal forest stands and implications for the measurement of the CO_2 flux. Agric. For. Meteorol. 140, 322–337.

Barr, A.G., Black, T.A., Hogg, E.H., Griffis, T., Morgenstern, K., Theede, A., Nesic, Z., 2007. Climatic controls on the carbon and water balances of a boreal aspen forest, 1994–2003. Global Change Biol. 12, 1–16.

Beer, C., Reichstein, M., Tomelleri, E., Ciais, P., Jung, M., Carvalhais, N., Rödenbeck, C., Arain, M.A., Baldocchi, D., Bonan, G.B., Bondeau, A., Cescatti, A., Lasslop, G., Lindroth, A., Lomas, M., Luyssaert, S., Margolis, H., Oleson, K.W., Roupsard, O., Veenendaal, E., Viovy, N., Williams, C., Woodward, F.I., Papale, D., 2010. Terrestrial gross carbon dioxide uptake: global distribution and covariation with climate. Science, http://dx.doi.org/10.1126/science.1184984.

Belcher, S.E., Finnigan, J.J., Harman, I.N., 2008. Flows through forest canopies in complex terrain. Ecol. Appl. 18, 1436–1453.

Bergeron, O., Margolis, H.A., Black, T.A., Coursolle, C., Dunn, A.L., Barr, A.G., Wofsy, S.C., 2007. Comparison of CO_2 fluxes over three boreal black spruce forests in Canada. Global Change Biol. 13, 89–107, http://dx.doi.org/10.1111/j.1365680 2486.2006.01281.x.

Black, T.A., den Hartog, G., Neumann, H.H., Blanken, P.D., Yang, P.C., Russell, C., Nesic, Z., Lee, X., Chen, S.G., Staebler, R., Novak, M.D., 1996. Annual cycles of water vapour and CO_2 fluxes in and above a boreal aspen forest. Global Change Biol. 2, 219–229.

Canepa, E., Georgieva, E., Manca, G., Feigenwinter, C., 2010. Application of a mass consistent flow model to study the CO_2 mass balance of forests. Agric. For. Meteorol. 150, 712–723.

Cook, B.D., Davis, K.J., Wang, W., Desai, A.R., Berger, B.W., Teclaw, R.M., Martin, J.G., Bolstad, P.V., Bakwin, P.S., Yi, C., Heilman, W., 2004. Carbon exchange and venting anomalies in an upland deciduous forest in northern Wisconsin, USA. Agric. For. Meteorol. 126 (3–4), 271–295, http://dx.doi.org/10.1016/j.agrformet.2004.06.008.

Davis, K.J., 2008. Integrating field measurements with flux tower and remote sensing data. In: Hoover, Coeli M (Ed.), Field Measurements for Landscape-Scale Forest Carbon Monitoring. XVIII, 242 p. 20 illus., Hardcover. ISBN: 978-1-4020-8505-5.

Desai, A.R., Bolstad, P.V., Cook, B.D., Davis, K.J., Carey, E.V., 2005. Comparing net ecosystem exchange of carbon dioxide between an old-growth and mature forest in the upper Midwest, USA. Agric. For. Meteorol. 128 (1–2), 33–55, http://dx.doi.org/10.1016/j.agrformet.2004.09.005.

Dunn, A.L., Barford, C.C., Wofsy, S.C., Goulden, M.L., Daube, B.C., 2007. A long-term record of carbon exchange in a boreal black spruce forest: means, responses to interannual variability, and decadal trends. Global Change Biol. 13, 577–590.

Falge, E., Baldocchi, D., Olson, R.J., Anthoni, P., Aubinet, M., Bernhofer, C., Burba, G., Ceulemans, R., Clement, R., Dolman, H., Granier, A., Gross, P., Grünwald, T., Hollinger, D., Jensen, N.-O., Katul, G., Keronen, P., Kowalski, A., Ta Lai, C., Law, B.E., Meyers, T., Moncrieff, J., Moors, E., Munger, J.W., Pilegaard, K., Rannik, Ü., Rebmann, C., Suyker, A., Tenhunen, J., Tu, K., Verma, S., Vesala, T., Wilson, K., Wofsy, S., 2001. Gap filling strategies for defensible annual sums of net ecosystem exchange. Agric. For. Meteorol. 107, 43–69.

Feigenwinter, C., Bernhofer, C., Vogt, R., 2004. The influence of advection on short-term CO_2 budget in and above a forest canopy. Boundary-Layer Meteorol. 113, 201–224.

Feigenwinter, C., Bernhofer, C., Eichelmann, U., Heinesch, B., Hertel, M., Janous, D., Kolle, O., Lagergren, F., Lindroth, A., Minerbi, S., Moderow, U., Mölder, M., Montagnani, L., Queck, R., Rebmann, C., Vestin, P., Yernaux, M., Zeri, M., Ziegler, W., Aubinet, M., 2008. Comparison of horizontal and vertical advective CO_2 fluxes at three forest sites. Agric. For. Meteorol. 148, 12–24.

Flanagan, L.B., Adkinson, A.C., 2011. Interacting controls on productivity in a northern Great Plains grassland and implications for response to ENSO events. Global Change Biol., http://dx.doi.org/10.1111/j. 1365-2486.2011.02461.x.

Flanagan, L.B., Syed, K.H., 2011. Stimulation of both photosynthesis and respiration in response to warmer and drier conditions in a boreal peatland ecosystem. Global Change Biol. 17, 2271–2287, http://dx.doi.org/10.1111/j. 1365-2486.2010.02378.x.

Finnigan, J., 2000. Turbulence in plant canopies. Annu. Rev. Fluid Mech. 32, 519–571.

Finnigan, J.J., 2008. An introduction to flux measurements in difficult conditions. Ecol. Appl. 18, 1340–1350.

Fischer, M.L, Billesbach, D.P., Riley, W.J, Berry, J.A., Torn, M.S., 2007. Spatiotemporal variations in growing season exchanges of CO_2, H_2O, and sensible heat in agricultural fields of the Southern Great Plains. Earth Interact., 11, Paper 17, 21.

Foken, T., Wichura, B., 1996. Tools for quality assessment of surface-based flux measurements. Agric. For. Meteorol. 78, 83–105.

Goulden, M.L., Munger, J.W., Fan, S.-M., Daube, B.C., Wofsy, S.C., 1996. Measurements of carbon sequestration by long-term eddy covariance: methods and a critical evaluation of accuracy. Global Change Biol. 2, 169–182.

Gu, L., Falge, E., Boden, T., Baldocchi, D.D., Black, T.A., Saleska, S.R., Suni, T., Vesala, T., Wofsy, S., Xu, L., 2005. Objective threshold determination for nighttime eddy flux filtering. Agric. For. Meteorol. 128, 179–197.

Gu, L.H, Meyers, T., Pallardy, S.G., Hanson, P.J., Yang, B., Heuer, M., Hosman, K.P., Riggs, J.S., Sluss, D., Wullschleger, S.D., 2006. Direct and indirect effects of atmospheric conditions and soil moisture on surface energy partitioning revealed by a prolonged drought at a temperate forest site, J. Geophys. Res. Atm., 111 (D16) Art. Num. D16102.

Gu, L.H., Massman, W.J., Leuning, L., Pallardy, S.G., Meyers, T., Hanson, P.J., Riggs, J.S., Hosman, K.P., Yang, B., 2012. The fundamental equation of eddy covariance and its application in flux measurements. Agric. For. Meteorol. 152, 135–148.

Heinesch, B., Yernaux, Y., Aubinet, M., 2008. Dependence of CO_2 advection patterns on wind direction on a gentle forested slope. Biogeosciences 5, 657–668.

Hollinger, D.Y., Kelliher, F.M., Byers, J.N., Hunt, J.E., McSeveny, T.M., Weir, P.L., 1994. Carbon dioxide exchange between an undisturbed old-growth temperate forest and the atmosphere. Ecology 75, 134–150.

Hollinger, D.Y., Aber, J., Dail, B., Davidson, E.A., Goltz, S.M., Hughes, H., Leclerc, M.Y., Lee, J.T., Richardson, A.D., Rodrigues, C., Scott, N.A., Achuatavarier, D., Walsh, J., 2004. Spatial and temporal variability in forest-atmosphere CO_2 exchange. Global Change Biol. 10, 1689–1706.

Humphreys, E.R., Black, T.A., Morgenstern, K., Cai, T., Drewitt, G.B., Nesic, Z., 2006. Carbon dioxide fluxes in three coastal Douglas-fir stands at different stages of development after harvesting. Agric. For. Meteorol. 140, 6–22.

Irvine, J., Law, B.E., Kurpius, M., 2005. Coupling of canopy gas exchange with root and rhizosphere respiration in a semi-arid forest. Biogeochemistry 73, 271–282.

Janssens, I.A., Lankreijer, H., Matteucci, G., Kowalski, A.S., Buchmann, N., Epron, D., Pilegaard, K., Kutsch, W., Longdoz, B., Grunwald, T., Montagnani, L., Dore, S., Rebmann, C., Moors, E.J., Grelle, A., Rannik, U., Morgenstern, K., Oltchev, S., Clement, R., Gudmundsson, J., Minerbi, S., Berbigier, P., Ibrom, A., Moncrieff, J., Aubinet, M., Bernhofer, C., Jensen, N.O., Vesala, T., Granier, A., Schulze, E.-D., Lindroth, A., Dolman, A.J., Jarvis, P.G., Ceulemans, R., Valentini, R., 2001. Productivity overshadows temperature in determining soil and ecosystem respiration across European forests. Global Change Biol. 7, 269–278, http://dx.doi.org/10.1046/j. 1365-2486.2001.00412.x.

Krishnan, P., Black, T.A., Barr, A.G., Gaumont-Guay, D., Grant, N., Nesic, Z., 2008. Factors controlling the interannual variability in the carbon balance of a southern boreal black spruce forest. J. Geophys. Res. 113, D09109, http://dx.doi.org/10.1029/2007JD008965.

Launiainen, S., Vesala, T., Molder, M., Mammarella, I., Smolander, S., Rannik, U., Kolari, P., Hari, P., Lindroth, A., Katul, G.G., 2007. Vertical variability and effect of stability on turbulence characteristics down to the floor of a pine forest. Tellus 59B, 919–936.

Law, B.E., Thornton, P., Irvine, J., Anthoni, P., Van Tuyl, S., 2001. Carbon storage and fluxes in ponderosa pine forests at different developmental stages. Global Change Biol. 7, 755–777.

Law, B.E., 2006. Carbon dynamics in response to climate and disturbance: recent progress from multi-scale measurements and modeling in AmeriFlux. In: Yamamoto, S. (Ed.), Plant Responses to Air Pollution and Global Change. Springer, Tokyo, Japan.

Law, B.E., Ryan, M.G., Anthoni, P.M., 1999. Seasonal and annual respiration of a ponderosa pine ecosystem. Global Change Biol. 5, 169–182.

Leuning, R., Zegelin, S.J., Jones, K., Keith, H., Hughes, D., 2008. Measurement of horizontal and vertical advection of CO_2 within a forest canopy. Agric. For. Meteorol. 148, 1777–1797.

Loescher, H.W., Law, B.E., Mahrt, L., Hollinger, D.Y., Campbell, J., Wofsy, S.C., 2006. Uncertainties in- and interpretation of carbon flux estimates using the eddy covariance technique. J. Geophys. Res. 111, D21S90.

Lund, R., Reeves, J., 2002. Detection of undocumernted change-points: a revision of the two-phase regression model. J. Climate 15, 2547–2554.

Luo, H., Oechel, W.C., Hastings, S.J., Zulueta, R., Qian, Y., Kwon, H., 2007. Mature semiarid chaparral ecosystems can be a significant sink. Global Change Biol. 13, 386–396, http://dx.doi.org/10.1111/j. 1365-2486.2006.01299.x.

Ma, S., Baldocchi, D.D., Xu, L., Hehn, T., 2007. Interannual variability in carbon dioxide exchange of an oak/grass savanna and open grassland in California. Agric. For. Meteorol. 147, 157–171, http://dx.doi.org/10.1016/j.agrformet.2007.07.008.

Mahecha, M.D., Reichstein, M., Carvalhais, N., Lasslop, G., Lange, H., Seneviratne, S.I., Vargas, R., Ammann, C., Arain, M.A., Cescatti, A., Janssens, I.A., Migliavacca, M., Montagnani, L., Richardson, A.D., 2010. Global convergence in the temperature sensitivity of respiration at ecosystem level. Science 329 (5993), 838–840, http://dx.doi.org/10.1126/science.1189587.

Mahrt, L., 1998. Flux sampling errors for aircraft and towers. J. Atmos. Oceanic Technol. 15, 416–429.

Marcolla, B., Cescatti, A., Montagnani, L., Manca, G., Kerschbaumer, G., Minerbi, S., 2005. Role of advective fluxes in the carbon balance of an alpine coniferous forest. Agric. For. Meteorol. 130, 193–206.

Massman, W.J., Lee, X., 2002. Eddy covariance flux corrections and uncertainties in long term studies of carbon and energy exchanges. Agric. For. Meteorol. 113, 121–144.

McCaughey, J.H., Pejam, M.R., Arain, M.A., Cameron, D.A., 2006. Carbon dioxide and energy fluxes from a boreal mixedwood forest ecosystem in Ontario, Canada. Agric. For. Meteorol. 140, 79–96.

Moffat, A.M., Papale, D., Reichstein, M., Hollinger, D.Y., Richardson, A.D., Barr, A.G., Beckstein, C., Braswell, B.H., Churkina, G., Desai, A.R., Falge, E., Gove, J.H., Heimann, M., Hui, D., Jarvis, A.J., Kattge, J., Noormets, A., Stauch, V.J., 2007. Comprehensive comparison of gap filling techniques for eddy covariance net carbon fluxes. Agric. For. Meteorol. 147, 209–232.

Monson, R.K., Sparks, J.P., Rosenstiel, T.N., Scott-Denton, L.E., Huxman, T.E., Harley, P.C., Turnipseed, A.A., Burns, S.P., Backlund, B., Hu, J., 2005. Climatic influences on net ecosystem CO_2 exchange during the transition from wintertime carbon source to springtime carbon sink in a high-elevation, subalpine forest. Oecologia 146, 130–147.

Montagnani, L., Manca, G., Canepa, E., Georgieva, E., Acosta, M., Feigenwinter, C., Janous, D., Kerschbaumer, G., Lindroth, A., Minach, L., Minerbi, S., Mö lder, M., Pavelka, M., Seufert, G., Zeri, M., Ziegler, W., 2009. A new mass conservation approach to the study of CO_2 advection in an alpine forest. J. Geophys. Res. 114, D07306, http://dx.doi.org/10.1029/2008JD010650.

Morgenstern, K., Black, T.A., Humphreys, E.R., Griffis, T.J., Drewitt, G.B., Cai, T., Nesic, Z., Spittlehouse, D.L., Livingston, N.J., 2004. Sensitivity and uncertainty of the carbon balance of a pacific northwest Douglas-fir forest during an El Nino/La Nina cycle. Agric. For. Meteorol. 123, 201–219, 10.1016/j.agrformet.2003.12.003.

Nave, L.E., Gough, C.M., Maurer, K.D., Bohrer, G., Hardiman, B.S., Le Moine, J., Munoz, A.B., Nadelhoffer, K.J., Sparks, J.P., Strahm, B.D., Vogel, C.S., Curtis, P.S., 2011. Disturbance and the resilience of coupled carbon and nitrogen cycling in a north temperate forest. J. Geophys. Res. 116, G04016, http://dx.doi.org/10.1029/2011JG001758.

Nemitz, E., Loubet, B., Lehmann, B.E., Cellier, P., Neftel, A., Jones, S.K., Hensen, A., Ihly, B., Tarakanov, S.V., Sutton, M.A., 2009. Turbulence characteristics in grassland canopies and implications for tracer transport. Biogeosciences 6, 1519–1537.

Ohtaki, E., 1984. Application of an infrared carbon dioxide and humidity instrument to studies of turbulent transport. Boundary-Layer Meteorol. 29, 85–107.

Oren, R., Hsieh, C.-I., Stoy, P., Albertson, J.A., McCarthy, H.R., Harrell, P., Katul, G.G., 2006. Estimating the uncertainty in annual net ecosystem carbon exchange:

spatial variation in turbulent fluxes and sampling errors in eddy-covariance measurements. Global Change Biol. 12, 883–896.
Papale, D., Reichstein, M., Aubinet, M., Canfora, E., Bernhofer, C., Longdoz, B., Kutsch, W., Rambal, S., Valentini, R., Vesala, T., Yakir, D., 2006. Towards a standardized processing of Net Ecosystem Exchange measured with eddy covariance technique: algorithms and uncertainty estimation. Biogeosciences 3, 571–583.
Piao, S., Ciais, P., Friedlingstein, P., Peylin, P., Reichstein, M., Luyssaert, S., Margolis, H., Fang, J., Barr, A., Chen, A., Grelle, A., Hollinger, D., Laurila, T., Lindroth, A., Richardson, A.D., Vesala, T., 2008. Net carbon dioxide losses of northern ecosystems in response to autumn warming. Nature 451 (7174), 49–53.
Post, W.M., Izaurralde, R.C., Jastrow, J.D., McCarl, B.A., Amonette, J.E., Bailey, V.L., Jardine, P.M., West, T.O., Zhou, J., 2004. Enhancement of carbon sequestration in U.S. soils. Bioscience 54, 895–908, http://dx.doi.org/10.1641/0006-3568(2004)054[0895:EOCSIU2.0.CO;2].
Reichstein, M., Falge, E., Baldocchi, D., Papale, D., Aubinet, M., Berbigier, P., Bernhofer, C., Buchmann, N., Gilmanov, T., Granier, A., Grunwald, T., Havrankova, K., Ilvesniemi, H., Janous, D., Knohl, A., Laurila, T., Lohila, A., Loustau, D., Matteucci, G., Meyers, T., Miglietta, F., Ourcival, J.-M., Pumpanen, J., Rambal, S., Rotenberg, E., Sanz, M., Tenhunen, J., Seufert, G., Vaccari, F., Vesala, T., Yakir, D., Valentini, R., 2005. On the separation of net ecosystem exchange into assimilation and ecosystem respiration: review and improved algorithm. Global Change Biol. 11, 1424–1439, http://dx.doi.org/10.1111/j. 1365-2486.2005.001002.x.
Reichstein, M., Ciais, P., Papale, D., Valentini, R., Running, S., Viovy, N., Cramer, W., Granier, A., Ogee, J., Allard, V., Aubinet, M., Bernhofer, C., BuchmannN, Carrara, A., GrunwaldT, Heimann, M., HeineschB, Knohl, A., KutschW, Loustau, D., Manca, G., Matteucci, G., Miglietta, F., Ourcival, J.M., Pilegaard, K., Pumpanen, J., Rambal, S., Schaphoff, S., Seufert, G., Soussana, J.F., SanzMJ, Vesala, T., Zhao, M., 2007a. Reduction of ecosystem productivity and respiration during the European summer 2003 climate anomaly: a joint flux tower, remote sensing and modelling analysis. Global Change Biol. 13, 634–651, http://dx.doi.org/10.1111/j. 1365-2486.2006.01224.x.
Reichstein, M., Papale, D., Valentini, R., Aubinet, M., Bernhofer, C., Knohl, A., Laurila, T., Lindroth, A., Moors, E., Pilegaard, K., Seufert, G., 2007b. Determinants of terrestrial ecosystem carbon balance inferred from European eddy covariance flux sites. Geophys. Res. Lett. 34, http://dx.doi.org/10.1029/2006GL027880.
Richardson, A.D., Hollinger, D.Y., Burba, G.G., Davis, K.J., Flanagan, L.B., Katul, G.G., Munger, J.W., Ricciuto, D.M., Stoy, P.C., Suyker, A.E., Verma, S.B., Wofsy, S.C., 2006. A multi-site analysis of random error in tower-based measurements of carbon and energy fluxes. Agric. For. Meteorol 136 (1–18), http://dx.doi.org/10.1016/j.agrformet.2006.01.00.
Richardson, A.D., Hollinger, D.Y., Aber, J., Ollinger, S.V., Braswell, B., 2007. Environmental variation is directly responsible for short- but not longterm variation in forest-atmosphere carbon exchange. Global Change Biol. 13, 788–803.
Richardson, A.D., Hollinger, D.Y., Dail, D.B., Lee, J.T., Munger, J.W., O'Keefe, J., 2009. Influence of spring phenology on seasonal and annual carbon balance in two contrasting New England forests. Global Change Biol. 29, 321–331.
Richardson, A.D., Black, T.A., Ciais, P., Delbart, N., Friedl, M.A., Gobron, N., Hollinger, D.Y., Kutsch, W.L., Longdoz, B., Luyssaert, S., Migliavacca, M., Montagnani, L., Munger, J.W., Moors, E., Piao, S., Rebmann, C., Reichstein, M., Saigusa, N., Tomelleri, E., Vargas, R., Varlagin, A., 2010. Influence of spring and autumn phenological transitions on forest ecosystem productivity. Philos. Trans. R. Soc., Ser. B 365, 3227–3246, http://dx.doi.org/10.1098/rstb.2010.0102.
Roulet, N.T., Lafleur, P.M., Richard, P.J.H., Moore, T.R., Humphreys, E.R., Bubier, J., 2007. Contemporary carbon balance and late Holocene carbon accumulation in a northern peatland. Global Change Biol. 13, 397–411.
Running, S.W., Baldocchi, D.D., Turner, D., Gower, S.T., Bakwin, P., Hibbard, K., 1999. A global terrestrial monitoring network, scaling tower fluxes with ecosystem modeling and EOS satellite data. Remote Sens. Environ. 70, 108–127, http://dx.doi.org/10.1016/S0034-4257(99)00061-9.
Saleska, S.R., Miller, S.D., Matross, D.M., Goulden, M.L., Wofsy, S.C., da Rocha, H.R., de Camargo, P.B., Crill, P., Daube, B.C., de Freitas, H.C., Hutyra, L., Keller, M., Kirchhoff, V., Menton, M., Munger, J.W., Pyle, E.H., Rice, A.H., Silva, H., 2003. Carbon in Amazon forests: unexpected seasonal fluxes and disturbanceinduced losses. Science 302, 1554.
Schwalm, C.A., Williams, C.A., Schaefer, K., Anderson, R., Arain, M.A., Baker, I., Barr, A., Black, T.A., Chen, G., Chen, J.M., Ciais, P., Davis, K.J., Desai, A., Dietze, M., Dragoni, D., Fischer, M.L., Flanagan, L.B., Grant, R., Gu, L., Hollinger, D., Izaurralde, R.C., Kucharik, C., Lafleur, P., Law, B.E., Li, L., Li, Z., Liu, S., Lokupitiya, E., Luo, Y., Ma, S., Margolis, H., Matamala, R., McCaughey, H., Monson, R.K., Oechel, W.O., Peng, C., Poulter, B., Price, D.T., Riciutto, D.M., Riley, W., Sahoo, A.K., Sprintsin, M., Sun, J., Tian, H., Tonitto, C., Verbeeck, H., Verma, S.B., 2010. A model-data intercomparison of CO_2 exchange across North America: results from the North American Carbon Program Site Synthesis. J. Geophys. Res. 115, G00H05, http://dx.doi.org/10.1029/2009JG001229.
Sellers, P.J., Hall, F.G., Kelly, R.D., Black, A., Baldocchi, D., Berry, J., Margolis, H., Ryan, M., Ranson, J., Crill, P., Lettenmaier, D., Cihlar, J., Newcomer, J., Halliwell, D., Fitzjarrald, D., Jarvis, P., Gower, S., Williams, D., Goodison, B., Wickland, D., Guertin, F., 1997. Boreas in 1997: scientific results; experimental overview and future directions. J. Geophys. Res., 102, 28,731–28, 770. doi:10.1029/97JD03300.
Schmid, H.P., Grimmond, C.S.B., Cropley, F., Offerle, B., Su, H.B., 2000. Measurements of CO_2 and energy fluxes over a mixed hardwood forest in the midwestern United States. Agric. For. Meteorol. 103, 357–374.
Solow, A.R., 1987. Testing for climate change: an application of the two-phase regression model. J. Climate Appl. Meteor. 26, 1401–1405.
Staebler, R.M., Fitzjarrald, D.R., 2004. Observing subcanopy CO_2 advection. Agric. For. Meteorol. 122, 139–156.
Staebler, R.M., Fitzjarrald, D.R., 2005. Measuring canopy structure and the kinematics of subcanopy flows in two forests. J. Appl. Meteorol. 44, 1161–1179.
Stoy, P.C., Katul, G.G., Siqueira, M.B.S., Juang, J-Y., Novick, K.A., Uebelherr, J.M., Oren, R., 2006. An evaluation of methods for partitioning eddy covariance-measured net ecosystem exchange into photosynthesis and respiration. Agric. For. Meteorol. 141, 2–18.
Sulman, B.N., Desai, A.R., Cook, B.D., Saliendra, N., Mackay, D.S., 2009. Contrasting carbon dioxide fluxes between a drying shrub wetland in Northern Wisconsin, USA, and nearby forests. Biogeosciences 6, 1115–1126.
Sun, J., Desjardins, R., Mahrt, L., MacPherson, J.I., 1998. Transport of carbon dioxide, water vapor and ozone by turbulence and local circulations. J. Geophys. Res. 103, 25873–25885.
Sun, H., Clark, T.L., Stull, R.B., Black, T.A., 2006. Two-dimensional simulation of airflow and CO_2 transport over a forested mountain. Part I. Interactions between thermally forced circulations. Agric. For. Meteorol. 140, 338–351.
Suyker, A.E., Verma, S.B., 2010. Coupling of carbon dioxide and water vapor exchanges of irrigated and rainfed maize-soybean cropping systems and water productivity. Agric For. Meteorol. 150, 553–563.
Suyker, A.E., Verma, S.B., Burba, G.G., 2003. Interannual variability in net CO_2 exchange of a native tallgrass prairie. Global Change Biol. 9, 255–265.
Urbanski, S, Barford, C., Wofsy, S., Kucharik, C., Pyle, E., Budney, J., McKain, K., Fitzjarrald, D., Czikowsky, M., Munger, J.W., 2007. Factors controlling CO2 exchange on timescales from hourly to decadal at Harvard Forest, J. Geophys. Res., 112 (G2), art. no. G02020.
Valentini, R., Matteucci, G., Dolman, A.J., Schulze, E.-D., Rebmann, C., Moors, E.J., Granier, A., Gross, P., Jensen, N.O., Pilegaard, K., Lindroth, A., Grelle, A., Bernhofer, C., Gŕunwald, T., Aubinet, M., Ceulemans, R., Kowalski, A.S., Vesala, T., Rannik, Ü., Berbigier, P., Loustau, D., Gu, J., Thorgeirsson, H., Ibrom, A., Morgenstern, K., Clement, R., Moncrieff, J., Montagnani, L., Minerbi, S., Jarvis, P.G., 2000. Respiration as the main determinant of carbon balance in European forests. Nature 404, 861–865, http://dx.doi.org/10.1038/35009084.
van Gorsel, E., Leuning, R., Cleugh, H.A., Keith, H., Suni, T., 2007. Nocturnal carbon efflux: reconciliation of eddy covariance and chamber measurements using an alternative to the u*-threshold filtering technique. Tellus 59B, 397–403.
van Gorsel, E., Leuning, R., Cleugh, H.A., Keith, H., Kirschbaum, M.U.F., Suni, T., 2008. Application of an alternative method to derive reliable estimates of nighttime respiration from eddy covariance measurements in moderately complex topography. Agric. For. Meteorol. 148, 1174–1180.
van Gorsel, E., Delpierre, N., Leuning, R., Black, A., Munger, J.W., Wofsy, S., Aubinet, M., Feigenwinter, C., Beringer, J., Bonal, D., Chen, B., Chen, J., Clement, R., Davis, K.J., Desai, A.R., Dragoni, D., Etzold, S., Grunwald, T., Gu, L., Heinesch, B., Hutyra, L.R., Jans, W., Kutsch, W., Law, B.E., Leclerc, M.Y., Mammarella, I., Montagnani, L., Noormets, A., Rebmann, C., Wharton, S., 2009. Estimating nocturnal ecosystem respiration from the vertical turbulent flux and change in storage of CO_2. Agric. For. Meteorol. 149, 1919–1930.
van Gorsel, E., Harman, I.N., Finnigan, J.J., Leuning, R., 2011. Decoupling of air flow above and in plant canopies and gravity waves affect micrometeorological estimates of net scalar exchange. Agric. For. Meteorol. 151, 927–933.
Verma, S.B., Dobermann, A., Cassman, K.G., Walters, D.T., Knops, J.M., Arkebauer, T.J., Suyker, A.E., Burba, G.G., Amos, B., Yang, H., Ginting, D., Hubbard, K.G., Gitelson, A.A., Walter-Shea, E.A., 2005. Annual carbon dioxide exchange in irrigated and rainfed maize-based agroecosystems. Agric. For. Meteorol. 131, 77–96.
Vickers, D., Irvine, J., Martin, J.G., Law, B.E., 2012a. Nocturnal subcanopy flow regimes and missing carbon. Agric. For. Meteorol. 152, 101–108.
Vickers, D., Thomas, C., Pettijohn, C., Martin, J., Law, B.E., 2012b. Five years of carbon fluxes and inherent water-use efficiency at two semi-arid pine forests with different disturbance histories. Tellus B 64, 17159, http://dx.doi.org/10.3402/tellusb.v64i0.17159.
Wang, X.L., 2003. Comments on detection of undocumernted change-points: a revision of the two-phase regression model. J. Climate 16, 3383–3385.
Webb, E.K., Pearman, G.I., Leuning, R., 1980. Correction of flux measurements for density effects due to heat and water vapour transfer. Q. J. R. Meteorol. Soc. 106, 85–100.
Yi, C., Anderson, D.E., Turnipseed, E.A., Burns, S.P., Sparks, J.P., Stannard, D.I., Monson, R.K., 2008. The contribution of advective fluxes to net ecosystem exchange in a high-elevation, subalpine forest. Ecol. Appl. 18, 1379–1390.
Zha, T., Barr, A.G., Black, T.A., McCaughey, J.H., Bhatti, J., Hawthorne, I., Krishnan, P., Kidston, J., Saigusa, N., Shashkov, A., Nesic, Z., 2009. Carbon sequestration in boreal jack pine stands following harvesting. Global Change Biol. 15, 1475–1487.